The DOI for this manuscript is doi: 10.1175/2009JCLI3138.1

Simulations of the 2004 North American Monsoon: NAMAP2

D. S. Gutzler[1], L. N. Long[2], J. Schemm[3], S. Baidya Roy[4], M. Bosilovich[5], J. C. Collier[6], M. Kanamitsu[6], P. Kelly[7], D. Lawrence[8], M.-I. Lee[5,9], R. Lobato S.[12], B. Mapes[7], K. Mo[3], A. Nunes[6], E. A. Ritchie[10], J. Roads[6], S. Schubert[5], H. Wei[11] and G. J. Zhang[6]

[1]University of New Mexico, [2]Wyle Information Systems, [3]NOAA Climate Prediction Center, [4]University of Illinois, [5]NASA Goddard Space Flight Center, [6]Scripps Institution of Oceanography, [7]University of Miami, [8]National Center for Atmospheric Research, [9]University of Maryland/Baltimore County, [10]University of Arizona, [11]NOAA Environmental Modeling Center, USA; [12]Instituto Mexicano de Tecnología del Agua, Mexico

revised for publication in *Journal of Climate*

July 28, 2009

Corresponding author address: Dr. David S. Gutzler, Earth & Planetary Sciences Dept., MSC03-2040, University of New Mexico, Albuquerque, NM 87131.
Email: gutzler@unm.edu

ABSTRACT

The second phase of the North American Monsoon Model Assessment Project (NAMAP2) was carried out to provide a coordinated set of simulations from global and regional models of the 2004 warm season across the North American monsoon domain. This project follows an earlier assessment, called NAMAP, that preceded the 2004 field season of the North American Monsoon Experiment. Six global and four regional models are all forced with prescribed, time-varying ocean surface temperatures. Metrics for model simulation of warm season precipitation processes developed in NAMAP are examined that pertain to the seasonal progression and diurnal cycle of precipitation, monsoon onset, surface turbulent fluxes, and simulation of the low-level jet circulation over the Gulf of California. Assessment of the metrics is shown to be limited by continuing uncertainties in spatially-averaged observations, demonstrating that modeling and observational analysis capabilities need to be developed concurrently. Simulations of the CORE subregion of monsoonal precipitation in global models has improved since NAMAP, despite the lack of a proper low-level jet circulation in these simulations. Some regional models run at higher resolution still exhibit the tendency observed in NAMAP to overestimate precipitation in the CORE subregion; this is shown to involve both convective and resolved components of the total precipitation. The variability of precipitation in the Arizona/New Mexico (AZNM) subregion is simulated much better by the regional models compared with the global models, illustrating the importance of transient circulation anomalies (prescribed as lateral boundary conditions) for simulating precipitation in the northern part of the monsoon domain. This suggests that seasonal predictability derivable from lower boundary conditions may be limited in the AZNM subregion.

1. Introduction

The North American Monsoon Experiment (NAME) [*footnote:* a table of acronyms is included as an Appendix] was organized as an international effort to improve observations, modeling, and prediction of the warm season circulation regime across southwestern North America (NAME Science Working Group, 2004). NAME activities centered around an intensive field observation campaign in summer 2004. In support of this field-oriented process study, a suite of modeling activities has taken place before, during, and after the 2004 summer field campaign.

The modeling component of NAME is motivated by the need to develop improved dynamical simulations of the North American monsoon circulation, which has been an area of active research for many years. The ultimate goal of NAME is improvement in seasonal prediction across North America during the warm season, and the North American monsoon is viewed as an integral driver of the continental circulation in the summer. Furthermore, NAME is predicated on the hypothesis that improvements in monitoring and simulation of weather-scale phenomena associated with warm season precipitation, including the diurnal cycle, are a prerequisite to achieving skillful coupled dynamical predictions of the large-scale seasonal circulation. Hence "improvements in the ability of models to simulate the various components and time scales comprising the weather and climate of the North American Monsoon System [NAMS]" were considered central goals of NAME (NAME Science Working Group, 2004).

The challenges of characterizing warm season precipitation in this region of complex terrain are amply illustrated in the literature. Coarse horizontal resolution can provide a primary limitation on monsoon simulations (Yang et al. 2001), although some global models seem to capture the gross features of the summer precipitation maximum despite not resolving the details of topography (Arritt et al. 2000), and more recent (generally higher resolution) global atmospheric models demonstrate an improved ability to simulate the seasonal cycle of NAMS precipitation (Lin et al. 2008). Vertical resolution, especially near the surface, plays an important role in the low level jet circulation in the Gulf of California and the simulation of orographic

precipitation, as described further in Section 3e. Sensitivity studies regarding monsoonal precipitation and resolution in global models are still being carried out (e.g. Lee et al. 2007a; Collier and Zhang 2007).

Simulations of monsoonal precipitation in higher resolution regional models have been shown to be quite sensitive to the choice of convective parameterization (Gochis et al. 2002, 2003) and land surface treatments (Kanamitsu and Mo 2003). Model deficiencies in simulating the diurnal cycle of precipitation have been investigated by Lee et al. (2007b), in which detailed comparisons were made among convective parameterization schemes used in the atmospheric general circulation models (AGCMs) from NOAA and NASA centers, and by Collier and Zhang (2006) using an AGCM developed at the National Center for Atmospheric Research (NCAR). Further investigation by Lee et al. (2008) with a set of sensitivity experiments using the NOAA National Centers for Environmental Prediction (NCEP) AGCM highlighted the importance of the convection trigger mechanism and how it was implemented in the parameterization scheme for correct precipitation diurnal cycle over North America during the warm season.

These uncertainties in climatological simulations have hampered efforts to examine the sensitivity of regional models to changing boundary conditions (Small 2001; Xu and Small 2002; Fawcett et al. 2002). In turn, the inconsistent quality of model control simulations presents an obstacle to producing skillful dynamical seasonal predictions of the large-scale NAMS circulation, which as mentioned above is a primary motivation for the entire NAME project (NAME Science Working Group 2004; Higgins et al. 2006).

Motivated by the modeling challenges outlined above, a coordinated set of retrospective simulations of the 1990 summer season, called the NAME Model Assessment Project or NAMAP, was carried out prior to the NAME field campaign (Gutzler et al. 2004, 2005). Both global and regional models were represented in the NAMAP assessment. Much of the NAMAP analysis was focused on monthly means and on the spatial domain defined as "Tier 1" (Fig. 1a) in the NAME Science Plan (NAME Science Working Group 2004). Smaller subregions within Tier 1, denoted AZNM and CORE, were also defined for spatial averaging purposes.

One of the products of the NAMAP set of simulations was a set of goals for model simulation improvement, based on several important features of the seasonal evolution of the NAMS that seemed problematic. These goals were formulated in terms of metrics for subsequent simulations (Gutzler et al. 2004, 2005). The metrics included:

- Determination of observed monsoon onset within 1 week.
- Correct simulation of monthly averaged precipitation rates to within 20% throughout the diurnal cycle.
- Simulate the magnitude of the observed afternoon peak of latent and sensible heat fluxes to within 20% on a monthly averaged basis.
- Correct simulation of the position of the Gulf of California low-level jet with respect to the Gulf and the high topography to the east.

This article describes results from a post-field phase modeling assessment, denoted NAMAP2, which has been designed to extend the temporal and spatial limitations of NAMAP to consider other NAME-related regions and consider sub-monthly variability. Daily temporal resolution is clearly needed to address the NAMAP metric concerning monsoon onset, as well as many other diagnostic quantities of interest.

To some degree, success in achieving each of the NAMAP simulation metrics is inescapably limited by our ability to validate them. It is quite likely, for example, that surface fluxes are not known to within 20% across the NAME domain. Likewise, large scale fields of observed precipitation do not properly constrain the diurnal cycle; for this metric the challenge in validating models involves comparison of pointwise raingauge observations (Gochis et al. 2007) with model-generated gridcell values. The value of NAMAP2, therefore, is not so much in demonstrating that models are perfect, or which particular model performs best, for one summer season. This model assessment exercise should instead be considered a step in an ongoing process of simultaneously improving both modeling capabilities and observational analyses pertaining to the summer climate of southwestern North America. Progress on both fronts will be necessary to achieve NAME's ultimate goal of improving seasonal prediction skill.

2. NAMAP2 Models and Protocols

The NAMAP2 simulation period extends across the boreal warm season of 2004, when the NAME Enhanced Observation Period took place. NAMAP2 includes modeling groups that participated in the first round of NAMAP simulations as well as several additional groups running other models. Participants helped to design the modeling strategy and the common boundary conditions used in the simulation (Table 1).

Time-varying SST was the principal prescribed surface boundary condition for NAMAP2 simulations. Experience from the initial NAMAP exercise indicated that existing operational SST products tend to be considerably too cold in the Gulf of California. Some observational evidence (e.g. Mitchell et al. 2002) suggested that proper simulation of surface temperature in the Gulf might be critical for properly simulating sufficiently strong atmospheric moisture transport up the Gulf, although regional models do not consistently reproduce such sensitivity (Mo and Juang 2003). The need for better temporal and spatial SST resolution over the Gulf of California for NAMAP2 gave impetus for a new SST analysis at NCEP/CPC that merges in-situ observations with multi-platform satellite retrievals (Wang and Xie 2007), denoted MPM. Most of the NAMAP2 simulations used the MPM analysis; one modeling group ran their seasonal simulation twice, once with MPM as the ocean surface temperature boundary conditions and another with an operational SST analysis.

No standard was set for land surface models, and each modeling group picked its own land surface component. Model initial spinup times also varied considerably among the different groups, which can affect surface hydrology considerably. To some extent, the use of the NOAA Reanalysis-2 for land surface initial conditions by most (but not all) of the modeling groups mitigates soil moisture spinup issues.

NAMAP2 simulations were carried out by 6 global modeling groups and 4 regional modeling groups (summarized in Table 2; more complete information on the different models can be obtained from the NAMAP2 web page at URL http://www.eol.ucar.edu/projects/name/namap2). Three different simulations with CAM3 are included: CAM3a and CAM3c differ in their

prescribed SST treatment, while CAM3b was run with a different (finite volume) dynamical core and a revised land surface model (Lawrence et al. 2007). Note that a rather wide range of horizontal resolutions is utilized by the various models, including two global models (FVM and GEOS-5) run at resolutions considerably less than 1°, comparable to all the regional models except the highest resolution MM5 simulation (run at 15 km).

A key difference between the global and regional model protocols is the constraint provided by prescribed time-varying lateral boundary conditions for the regional models. These boundary values were provided by the AMIP-II reanalysis product (Kanamitsu et al. 2002). Global models generate their own large-scale circulations, driven in part by prescribed ocean temperatures. Thus comparing the global and regional model simulations provides a suggestion of the importance of the correct simulation of the large-scale circulation surrounding the monsoon domain, and how well the global models succeed in creating that circulation.

Participating modelers were requested to submit an agreed-upon list of variables with three-hourly resolution for archiving and analysis at the NOAA Climate Prediction Center. Output was submitted over an analysis domain that corresponded to the "Tier 2" region defined in the NAME Science Plan, which extends across southwestern North America from 10°N to 40°N in latitude, and 90°W to 120°W in longitude (thus slightly larger than the area plotted in Fig. 1). Spatial averages within the smaller NAME Tier I region are emphasized here, in particular the NAME CORE subregion in the heart of the NAMS domain and the AZNM subregion near the northernmost extent of the monsoonal regime (Fig. 1). These subregions have been used in many previous NAME-related diagnostic studies, including NAMAP. One new region, Tier 1.5, was defined for this analysis because NAMAP indicated that a common modeling flaw involved generating precipitation too far to the east relative to observations. Tier 1.5, with an area intermediate between NAME Tiers 1 and 2 (Fig. 1), was designed to capture such shifts in precipitation.

An online atlas of NAMAP2 results contains many more images of NAMAP2 results than are presented here. The online NAMAP2 atlas is hosted at the University of Miami at URL

http://www.rsmas.miami.edu/personal/pkelly/NAMAP2.html (also accessible via NCEP at http://www.cpc.ncep.noaa.gov/products/outreach/atlas.shtml). Additional results and analysis from the NAMAP2 simulations, emphasizing land surface fluxes, have been carried out by Kelly and Mapes (2009).

The metrics proposed in NAMAP are used to organize this overview of the NAMAP2 simulations, beginning with a description of the total warm season precipitation and the seasonal progression of the 2004 monsoon season. A more detailed discussion of monsoon onset follows the description of the seasonal cycle. The diurnal cycle of precipitation, surface fluxes, and regional low-level jet circulations are then examined, along with a brief discussion of precipitation frequency.

3. NAMAP2 Simulations of the 2004 North American Monsoon

a) Seasonal progression of observed precipitation

Improvements in the observation, simulation, and prediction of warm season precipitation are a special focus of NAME research. As an indication of the uncertainty in NAME-era estimates of precipitation, estimates of the total warm season rainfall (Jun-Sep 2004) from three observational products, none of which incorporates special NAME observations, are shown in Fig. 1. The URD product (Fig. 1a) is a 1°×1° analysis based only on gauge data (Higgins et al. 2000); RMORPH (Fig. 1b) is a blend of gauge data and satellite observations of longwave radiation (Janowiak et al. 2007); TRMM (Fig. 1c) is a radar-based satellite product (Huffman et al. 2000).

The general patterns of time averaged continental precipitation are similar between URD and RMORPH -- as indeed they should be considering that essentially the same rain gauge data are used for both analyses -- but URD tends to estimate higher values of precipitation. The difference between URD and RMORPH for this period is generally on the order of 10% across much of the area depicted, but in some subregions the difference between these two observational products approaches 20%, which is the NAMAP-specified metric for successful model simulation. The spatial pattern of precipitation in the TRMM data is broadly similar to

both the URD and RMORPH analyses, but TRMM estimates are systematically dryer (as shown by Gochis et al. 2009), producing additional spread among the observations.

Time series of the same three observed estimates of total monthly observed precipitation shown in Fig. 1 from May to September 2004, averaged over the CORE subregion (Fig. 2a, black lines), show the pronounced increase between June and July typical of the North American monsoon. In 2004 precipitation decreased in August relative to July. These results can be compared with precipitation derived from a network of rain gauges implemented during the 2004 NAME field season in several transects within the CORE subregion, as part of the NAME Event-based Raingauge Network (NERN; Gochis et al. 2007). The 86 rain gauges in the NERN dataset all fall into a region that corresponds closely to the CORE subregion, providing a spatial sample in this subregion considerably denser than the URD dataset. All rain gauges available during this period were weighted equally to create daily and monthly averages, as shown by the line labeled "NERN" in Fig. 2a. The NERN-derived monthly values are systematically higher than any of the other observational estimates, consistent with previous analyses (Gochis et al. 2009) that have demonstrated the low bias of existing operational precipitation products that underestimate orographic precipitation in data-sparse high elevation regions. Adding the NERN data here emphasizes the spread in existing estimates of precipitation, and reinforces the notion that model validation in the data-sparse core region of the North American monsoon domain is still limited by the quality and comprehensiveness of the observed data record.

b) Seasonal progression of simulated precipitation

All the simulations (both global and regional) except CAM3a reproduce an increase in total precipitation in the CORE subregion from June to July. This represents a marked improvement over the NAMAP simulations, for which the global models systematically delayed monsoon onset and thereby misrepresented the seasonal progression. The improvement in simulation results is consistent with the assessment of global atmospheric models presented by Lin et al. (2008). Among the global models, CAM3a and CAM3c stand out as drier in July compared to

the other models and observations. These two simulations initiate precipitation too far to the east; the seasonal progression of precipitation in these two simulations is closer to observations when rainfall is averaged across the larger Tier 1.5 region (Fig. 2c, as discussed below). The spread of CORE-averaged precipitation among global models increased in August, with four models continuing to increase precipitation from July to August, one model (CAM3a) initiating precipitation in August instead of July, and two models following the observed progression of a July peak followed by an August decrease.

All the regional models also simulate a large increase in CORE precipitation from June to July, and all models except MM5b then correctly exhibit a decrease in precipitation from July to August. As was the case in NAMAP, the MM5 simulations (red and light blue lines in Fig. 2a) tend to oversimulate precipitation in the CORE subregion. The reasons for the excess rainfall will be discussed below in conjunction with the diurnal cycle.

The seasonal progression in the more northern AZNM subregion is different in that precipitation continues to increase from July to August in each of the observed estimates after the initial large increase in July associated with monsoon onset (Fig. 2b). This seasonal progression is not uncommon in AZNM, where onset typically occurs later in the season than in the CORE region to the south (Higgins et al. 1997). Neither the global nor the regional models consistently capture the Jul-Aug precipitation increase.

The seasonal progression in Tier 1.5 is flatter from June through September compared with the seasonal cycle in CORE or AZNM (Fig. 2c). This is because observed precipitation in the eastern half of the Tier 1.5 box decreases as the western (monsoonal) part increases, as shown further below.

Overall, Fig. 2 shows that the models tend to exhibit nearly the same rank order (more to less precipitation) in each of the subregions shown. This suggests that the differences in precipitation amounts generated by the various models has more to do with model physical parameterization techniques (that could change the propensity for precipitation across the model domain) than

with shifts in large-scale circulation patterns that would shift maxima and minima in precipitation from one simulation to another.

Maps of total monthly precipitation in Fig. 3 show that the increase in precipitation from June to July in the CORE and AZNM subregions was accompanied by a decrease in precipitation in Texas and northeastern Mexico, east of the 100th meridian (Fig. 3a shows RMORPH observations). This opposition in seasonal progressions between the monsoon domain and the U.S. midwest is a well-known feature of North American precipitation (Higgins et al. 1997). Regional models tend to successfully simulate this opposition, as exemplified by the MM5a results in Fig. 3b, but global models are generally less successful in this regard (e.g. CFS results in Fig. 3c).

The presence of prescribed lateral boundary conditions for the regional model simulations is the probable cause of the improvement of this feature in the regional model simulations. Monthly mean wind observations at 850 hPa (from the North American Regional Reanalysis or NARR; Mesinger et al. 2006), superimposed on precipitation, show a pronounced decrease from June to July in the magnitude of onshore flow from the Gulf of Mexico in conjunction with the precipitation decrease across the southern U.S. plains (Fig. 4a). A similar monthly progression is simulated by MM5, with much smaller June-July monthly changes in both precipitation and winds simulated by CFS along the coast of the Gulf of Mexico.

Farther west in the CORE subregion, the pronounced increase in precipitation seen in Fig. 4 from June to July in the NARR analysis and both model simulations is difficult to correlate with any obvious changes in the monthly mean low level wind field. We shall return to this point in section 3e in the context of low-level jet circulations.

Daily time series of precipitation for observations and simulations, averaged over the CORE subregion, are shown in Fig. 5. Observed estimates are reproduced as black, grey, and brown lines in each panel and each model is represented by a different color. It is readily apparent that over the CORE region the URD and RMORPH observed estimates exhibit qualitatively similar daily fluctuations, with URD showing systematically higher amounts. The TRMM estimates are

considerably different on many days. The pronounced monthly increase in July precipitation compared to June discussed previously is easily evident in most of these time series plots, suggesting that the models are capturing the gross first-order feature of the seasonal progression. Not surprisingly, however, the global models driven only by prescribed SST exhibit little day-to-day correspondence between model simulations and observations. Regional models, also forced by prescribed lateral circulation, do capture some of the major transient events (e.g. major peaks in CORE rainfall around 12 July and 20 July) but also generate other rainfall maxima that do not exist in the data. The RSM regional model provides the best fit to the data.

Observed monsoon onset in the CORE subregion occurs on Jun 5, following the definition of Higgins et al. (1997) of three consecutive days of significant (1.5 mm/day) area-averaged rainfall (Table 3). As Fig. 5 shows, this onset date was associated with a transient rainfall event followed by dry conditions that persisted for several weeks. Nevertheless several models (both global and regional) matched this onset date rather closely; whether this indicates outstanding simulation skill or is just fortuitous is difficult to say. Overall, however, these results are highly encouraging with regard to the ability of global models to simulate monsoon onset with some fidelity in the CORE subregion.

Analogous time series for the AZNM subregion (Fig. 6) lead to similar conclusions although model fidelity to observations is worse. Observations indicate extremely dry conditions until late June, whereas most models simulate at least one significant transient rainfall event during that period. The observed onset date for AZNM (based on a 0.5 mm/d threshold) is Jul 11 (Table 3), but all simulations except GFS and RAMS generate an earlier onset date in June.

Tropical storm Blas passed the mouth of the Gulf of California on 12 July 2004 as it propagated northward along the west coast of Mexico. Monsoon onset in AZNM has been attributed to the moisture surge associated with Blas (Johnson et al. 2007). Most of the NAMAP2 simulations -- those with a horizontal resolution finer than 1° -- seemed to generate a tropical storm in the eastern Pacific at about this time (results not shown), although a detailed assessment of tropical storm dynamics in these simulations is beyond the scope of this paper.

Precipitation over both the CORE and AZNM regions generally increased in the model simulations following the observed dates when Blas affected the NAM region (Figs. 5, 6). However most models had already predicted an onset in early June, so the presence of Blas did not affect the calculation of the onset date in the simulations. It is encouraging however that the models successfully simulate tropical storms and their associated moisture surges. Many models also simulate moisture surges in the Gulf of California not associated with tropical storms.

Throughout July and August, global models systematically underestimate day-to-day variability in AZNM-averaged precipitation, producing less intense precipitation day after day. Regional models, in contrast, were much more realistic in simulating the transient character of AZNM precipitation (e.g. RSM and RAMS simulations). Each of the regional models depicted heavy rainfall days in July and August, separated by days with no precipitation. These results seem to confirm the importance of large-scale weather for dynamic enhancement or suppression of summer precipitation in the continental interior. Given the correct (prescribed) observed large-scale circulation around the periphery of the monsoon domain, regional models provide a much more faithful reproduction of intramonthly precipitation events compared to global models that do not contain regional scale circulation constraints.

c) Diurnal cycle of precipitation

The diurnal cycle of precipitation, averaged on a monthly basis over the CORE subregion, is shown for the months of Jun, Jul and Aug 2004 in Fig. 7. Collectively the global models (top panel) simulate reasonably well the diurnal cycle of total precipitation in the CORE subregion when compared to RMORPH or TRMM estimates [*footnote:* URD does not resolve the diurnal cycle in Mexico and is therefore not included here. The minor peaks at 00, 06, 12, and 18z in the RMORPH data are artifacts of its prototype gauge/satellite blending algorithm. An ambiguity arises when the hourly rain gauge input for a particular grid cell is non-zero but the corresponding satellite input is zero. To account for this "extra" daily rainfall, the gauge data are divided into fourths and added to the four main synoptic time periods: 00Z, 06Z, 12Z and 18Z.

Therefore, when looking at the hourly diurnal cycle of precipitation rate, these four hours may have artificial "bumps".]

In general the global models tend to underestimate the magnitude of the diurnal peak. All models except one capture the pronounced increase in precipitation from June to July, and simulate a sharp diurnal peak in precipitation near 00Z (1800 local time). Most models, however, show a sharper diurnal peak than the observations indicate, i.e. the average diurnal cycle drops off more sharply between 03Z and 09Z in the simulations than in the observations. Among the regional models (Fig. 7, bottom), the RSM model provides a very close simulation of the observations, while the two MM5 simulations overestimate considerably the observed rainfall rates throughout the diurnal cycle. [*footnote:* The RAMS regional model was excluded from the diurnal cycle analysis because of evident problems with its high-frequency output data set, but this does not impact the monthly averaged data derived from RAMS.]

Total precipitation in the CORE subregion is split into convective and resolved components in Fig. 8. Deep convection and stratiform rain are both important and significant across the CORE subregion (Williams et al. 2007). The diurnal cycle of CORE convective precipitation (Fig. 8, left panels) reaches a peak near 00Z in all models. The amplitude of convective precipitation varies considerably among the global models but is remarkably consistent among the regional models. The rate of resolved precipitation, i.e. rain from stratiform clouds simulated in the models via grid saturation or fractional cloudiness schemes, is much smaller in the global models (note that the ordinate in Fig 8b is greatly expanded relative to the other panels). In contrast, resolved precipitation in the regional models (Fig. 8d) is generally of equivalent amplitude to convective precipitation but varies greatly from one model to another. The large amount of resolved precipitation in the MM5 simulations accounts for much of the overestimate of total precipitation by these models noted previously in Fig. 2 and Fig. 7.

Models with higher spatial resolution should naturally represent a higher fraction of total precipitation as "resolved", so it is not surprising that the fraction of precipitation delivered via subgrid scale processes decreases as model resolution increases. However Fig. 8 suggests that

the transition from subgrid-scale thunderstorms to resolved precipitation is not just a simple tradeoff, and seems to pose problems for the MM5 simulations.

The diurnal cycle of total precipitation in the AZNM subregion (**Fig. 9**) is generally poorly represented compared to the CORE subregion. Observations indicate almost no precipitation in June, increasing sharply in July with a diurnal peak at 00Z that continues in August. There is a factor of 2 difference in the estimates of the diurnal peak between the RMORPH and TRMM products. The models present a huge spread of results, ranging from severe underestimates of July and August precipitation to simulations that tremendously overestimate the observed estimates, often with simulated diurnal peaks several hours later in the evening than the observations.

This wide range of simulated results is highlighted in the decomposition into convective vs. resolved rainfall in AZNM (Fig. 10). As was the case for CORE precipitation, nearly all of the rainfall in the global models is convective (Fig. 10a), whereas the regional models (especially the MM5 simulations) present a somewhat more even partitioning into convective and resolved components. Unlike the CORE subregion, the diurnal cycles in the different simulations exhibit a very large spread in terms of both magnitude and phase of convective precipitation. The AZNM subregion presents a less uniform geographical constraint on the development of convective thunderstorms compared to the CORE subregion, and the results in Fig. 10 demonstrate that convective precipitation still presents a huge challenge for models in AZNM.

d) Surface energy fluxes and temperature

Large-scale fields of surface energy fluxes are poorly constrained by available observations, and this general statement is particularly true in the data sparse NAMS region. Watts et al. (2007) carried out an assessment of land surface variability during the 2004 NAME field season across a transect of sites extending from the northern part of the CORE subregion northward to near the southern boundary of AZNM in Arizona. They documented large site-to-site differences associated with elevation and vegetation type that are not resolved by any of the NAMAP2

models. Here we compare spatial averages of surface fluxes, soil moisture and temperature from the model simulations with monthly values obtained from the NARR, which in the absence of surface observations is largely a model-generated product.

Soil moisture and surface temperature and fluxes in NARR should be strongly constrained by observed precipitation, which is assimilated in the analysis. Limitations and possible deficiencies in NARR surface values in the NAME region have been documented by Vivoni et al. (2008), however. Two of the NAMAP2 model systems -- the GFS global model and RSM regional model -- use the same land surface model (NOAH) employed in the NARR, so those models should be expected to reproduce NARR-generated surface variables rather closely.

The NARR values of sensible heat flux (SH) for the CORE subregion show a sharp month-to-month decrease from June to July to August (Fig. 11, black line in top two panels), and the latent heat flux (LH) increases over the same time span (middle panels), as would be expected during the transition from the spring dry season to the monsoon season. The sum of these fluxes SH+LH varies by a relatively small amount while the Bowen Ratio (SH/LH, bottom panels) decreases substantially as the monsoon season progresses.

All the global models, and the RSM regional model, also show a pronounced decrease in SH, and increase in LH, from June to August (Fig. 11). This general result does not agree with Watts et al.'s (2007) two observed flux sites in the northern part of the CORE subregion, which exhibit a decrease in evapotranspiration from July to August associated with a submonthly dry spell at those sites. Furthermore the spread of model-generated monthly averages of sensible flux (Fig. 11, top) and latent flux (Fig. 11, middle), averaged over the CORE subdomain, corresponds to the spread in precipitation shown in previous figures. Simulations exhibiting relatively low sensible flux (e.g. global GEOS5 and regional MM5b) also generate relatively high latent flux and large rainfall rates (Fig. 2) and high surface soil moisture (Fig. 13, discussed in more detail later) [*footnote:* MM5a surface fluxes and soil moisture were not submitted.] Differences in simulated surface fluxes can also be associated with corresponding precipitation differences, e.g. the CAM3a values of SH and LH do not change much until August, associated with the delayed

monsoon onset in this simulation (Fig. 2a). However the MM5b regional simulations show very little change in SH from May to July, and LH decreases from very high values in May despite a corresponding increase from May through July in precipitation (Fig. 2a).

Associated monthly time series of SH (top) and LH (bottom) for the AZNM subdomain are shown in Fig. 12. Sensible flux exhibits a steady decrease of about 40 W/m^2 in NARR data from May to Sep, and this is tightly reproduced by global models -- most of the spread among models is represented by a constant offset. Latent flux doubles from about 20 to about 40 W/m^2 on average, but the models exhibit considerably more spread in LH values, strongly correlated with the corresponding spread of monthly values of precipitation (Fig. 2b).

Among regional models, the monthly progression of RSM-simulated SH and LH fluxes stays within about 20% of NARR estimates (as expected), but the MM5b and RAMS simulations vary tremendously. There is much less correspondence between precipitation and surface flux variability in the regional models compared to the global models. A possible explanation for this difference is that the imposition of lateral circulation fluctuations may act to decouple precipitation from surface fluxes in the regional models. This would make it difficult to evaluate surface feedbacks with regional models.

Surface soil moisture (expressed as a fraction of soil water capacity) in NARR increases from June to August from about 0.15 to 0.3 in the CORE subregion, and from less than 0.15 to 0.2 in AZNM (Fig. 13). Most of the models (except RSM) exhibit less variability than NARR, i.e. the large increases in precipitation during the monsoon months do not dramatically affect surface soil moisture, potentially diminishing the amplitude of soil moisture feedbacks in the models (at least, compared to NARR). The GEOS5 and FVM global models exhibit much more soil moisture sensitivity than the other models. The MM5b simulation, which generated apparently excessive precipitation in both subregions (Fig. 2), does not maintain correspondingly excessive soil moisture as one would expect when looking at the heat fluxes.

The monthly averaged diurnal cycle of 2-m air temperature is shown in Fig. 14, with NARR data again used as an observational benchmark. The majority of global models exhibit

systematically higher temperature than NARR, especially during daytime, in both CORE (Fig. 14a) and AZNM (Fig. 14b) subregions. The spread among models is considerably greater in AZNM compared to CORE. The global models generally tend to be too warm at both the minimum and maximum points in the diurnal cycle, although CFS simulates cooler nocturnal temperatures than NARR in AZNM. Largest differences relative to NARR are associated with maximum temperatures, so the global models tend to overestimate the amplitude of the diurnal cycle. The regional models exhibit less spread, although the MM5 simulations (which overestimate precipitation) exhibit cooler temperatures, especially in AZNM.

e) Gulf of California Low Level Jet

As outlined in the Introduction, one of the modeling goals derived from the first NAMAP exercise was to improve simulation of the low level jet (LLJ) in the Gulf of California. The LLJ has been identified as an essential feature for moisture transport for the entire North American monsoon system precipitation in high resolution simulations (e.g. Stensrud et al. 1997; Berbery 2001). However coarse resolution models that do not properly resolve the Gulf of California, hence do not fully describe diurnal surface fluxes and horizontal pressure gradients across the Gulf, should not be expected to simulate the essential mesoscale features of the LLJ [*footnote:* Some coarse resolution models can partially reproduce the effects of the water surface via a subgrid scale surface classification scheme. All of the NAMAP2 models, except the CAM3 models, exhibit much enhanced surface moisture over the grid cells corresponding to the Gulf of California, even if those grid cells are not explicitly identified as having a water surface.] Most modeling studies of the LLJ have been carried out using higher resolution regional models (e.g. Stensrud et al. 1995; Anderson et al. 2000, 2001; Fawcett et al. 2002; Saleeby and Cotton 2004) that explicitly resolve the Gulf of California.

Current operational observational networks do not have sufficient temporal or spatial resolution to fully constrain predictive models of the mesoscale circulations in the Gulf of California. With this in mind, much of the enhanced observation system implemented during the

NAME 2004 field campaign was designed to capture the structure and variability of the LLJ (NAME Science Working Group 2004). Wind profiler observations from the northern Gulf of Mexico during the field campaign show a prominent time-averaged southerly jet, strongest during nocturnal hours (Johnson et al. 2007). Assimilated data from NARR for JJA 2004 reproduce a clear climatological jet at 925 hPa at 12Z (Fig. 15a). Consistent with previous studies of the summertime Gulf of California circulation, the low level flow turns onshore (i.e. southwesterly, upslope onto the Sierra Madre Occidental) at 00Z (Fig. 15b). The models tend to do a better job with this onshore flow at 00Z than at 12Z, as seen in both MM5 simulations, the FVM simulation, and the CFS/GFS simulations in the northern sector (not shown).

As mentioned above, coarse resolution models are not expected to capture this structure. As examples, JJA 12Z climatological wind vectors from CFS at 925 hPa (Fig. 15c; GFS was practically identical), and from the CAM3b simulation at 850 hPa (Fig. 15d) both show northwesterly flow down the Gulf. These winds represent the eastward extension of the Pacific subtropical anticyclone. This circulation structure helps explain why coarse resolution models tend to simulate less precipitation north of the Gulf of California in the AZNM subregion than higher resolution models (Fig. 2, and Fig. 3c for CFS).

High horizontal resolution, however, is not sufficient to generate southerly noctural low-level winds up the Gulf of California. The two NASA global models, FVM and GEOS5, both exhibit time-averaged 850 hPa winds with a northerly component at 12Z, despite being run at horizontal resolutions that clearly resolve the Gulf. Similarly, the RSM model, which is run at similarly high resolution but is heavily conditioned by the large-scale circulation generated by the global model in which it is embedded, fails to simulate southerly low-level winds in the Gulf of California (Fig. 15e).

However the high-resolution MM5 simulations do simulate a LLJ in the northern Gulf of California (Fig. 15f). These two simulations produced the most precipitation in both the CORE and AZNM subregions, considerably exceeding the observational estimates. However, the additional precipitation produced by these models can be accounted for in the resolved

precipitation (as discussed in Section 3b with the diurnal plots in Fig 8b) and is not due to subgrid scale precipitation.

f) Frequency of precipitation

Most previous studies of NAMS precipitation have focused on total rainfall amounts. Model simulations lend themselves to analysis of both rainfall rate and frequency, but comparison with observations (where observations exist) can be problematic. The ambiguities in analyzing precipitation frequency are illustrated by the observed frequencies for JJA 2004 for gridpoints within the CORE subregion derived from URD estimates (Fig. 16a) and TRMM estimates (Fig. 16b). In URD data, the overall daily mean is 3.5 mm/d. The mode (most frequent range of values) in the histogram of daily precipitation values is 0.1 to 2.5 mm/d. For the same months and spatial area, the overall mean of TRMM estimates is 2.1 mm/d, and the mode of the histogram is 0 (no rainfall) in a grid cell, which occurs about 45% of the time (the RMORPH-based histogram, not shown, is very similar). Just 15% of daily values in the URD data exhibit zero rainfall. The TRMM precipitation algorithm cuts off small subgrid scale rainfall amounts, leading to more days with zero precipitation on the grid scale compared to the gauge-based URD analysis.

Most of the NAMAP2 models exhibit a 'URD-style' distribution of daily precipitation rate across the CORE subregion, with relatively few zero daily values and a modal value on the order of 1 mm/d, similar to URD observations. A representative example of a model-generated histogram (from the NOAA CFS simulation) exhibits zero rain on 10-20% of JJA days (Fig. 16c). From histograms like these we find that most of the spread among models in total precipitation amount (Fig. 3) is associated with different maximum rain rates in the various models, and not so much from differences in daily precipitation frequency.

These results can be compared with precipitation frequencies derived from the NERN dataset discussed in Sec. 3a. The NERN data suggest that rainfall totals can increase by a factor of two or more from near-coastal areas along the Gulf of California to the higher elevations of the Sierra

Madre Occidental to the east (Gochis et al. 2007). These differences are due almost entirely to maximum daily precipitation rate, not to frequency of precipitation. The daily frequency of precipitation at individual raingauges is very close to 50% at nearly all the NERN sites, similar to the satellite-based precipitation products (RMORPH and TRMM). Thus the analysis of both observational data and the model assessment described here point to rainfall intensity as a primary source of uncertainty in precipitation estimation and simulation in the CORE subregion.

4. Discussion

The results presented in the previous section represent progress in simulating the North American monsoon since the NAMAP project (Gutzler et al. 2005), as well as illustrating the remaining challenges of simulating warm season rainfall and the climatic conditions that support the "rainy season" in this semiarid region. With just one exception, all the NAMAP2 simulations capture some semblance of a seasonal increase in precipitation from June to July in subregions of NAME Tier 1 (Fig. 2). As before, several of the simulations (both regional and global models) continue to generate increased rainfall from July to August in the CORE subregion, whereas observations indicate that rainfall in 2004 peaked in July (as is the case climatologically). Several of the models performed remarkably well -- within the envelope of uncertainty defined by different operational rainfall analysis products -- in tracking the observed seasonal cycle of area-averaged rainfall.

The separation of precipitation into convective and resolved components in Figs. 8 and 10 indicates that the treatment of precipitation, in terms of the overall amplitude and diurnal cycle, is occurring quite differently in the various models. Convective precipitation in the regional models run at high resolution was reasonably consistent from model to model, despite their use of different convective parameterizations. However the transition to resolved precipitation (several hours after the convective peak) was handled very differently in these models. Detailed diagnosis of the convective-to-resolved transition is beyond the scope of this study, but a conclusion of the analysis is that this transition deserves considerable further study. Clearly the

warm season precipitation challenge in the NAM region extends beyond merely improving convective parameterizations.

The global models, most of which were run at lower horizontal resolution, generally produced little or no resolved precipitation, so model-to-model differences (which are considerable) resulted from different treatments of moist convection, and/or from different simulations of flow and thermodynamic structure in the NAM region as part of their different global climates. To be effective, a modeling strategy that involves a regional model nested within a coarser global model obviously demands that the large scale structure generated by the global model be realistic. This point is reinforced by comparing the regional and global model seasonal progression of precipitation (Fig. 2), which strongly indicates that the prescribed large-scale lateral boundary conditions play a key role in determining the seasonal progression of the monsoon.

There is no evident systematic relationship between a model's ability to simulate the LLJ and its corresponding simulation of warm season precipitation amount (Fig. 15). We have suggested that sufficient model resolution is necessary but not sufficient to simulate the LLJ, but the large-scale monsoonal circulation resolved by the models generates a reasonable seasonal progression of precipitation (Fig. 2), even in the absence of a correct mesoscale LLJ circulation. The models that simulate apparently reasonable precipitation rates in the CORE subregion generate an upslope afternoon circulation onto the Sierra Madre mountains without a LLJ transporting moisture up the Gulf of California. We should not expect models to realize whatever predictability may be tied to the LLJ and its variability (such as surge events; Higgins et al. 2004), although the general seasonal progression and diurnal cycle are reasonably simulated by current models.

NAMAP and NAMAP2 emphasized assessment hindcast simulations of warm season circulation features. As such these assessments do not directly address the seasonal predictability of the North American monsoon circulation and rainfall. Nevertheless we can draw some working hypotheses from the results that might be considered in future predictability studies.

First, we hypothesize that long-lead predictability should be greater in the CORE subregion compared to the AZNM subregion. The very highly transient nature of warm season precipitation on the far northern fringe of the monsoon circulation, and the evident importance of time-dependent lateral boundary conditions that gave the regional models such an advantage over the global models for simulating rainy episodes, suggests that potentially predictable oceanic boundary conditions may be more important for determining rainfall in the CORE subregion.

This hypothesis would seem to be at odds with the existing literature on seasonal prediction of the monsoon, which to date has emphasized predictability within the United States based on empirical studies of antecedent land surface conditions (e.g. Gutzler 2000) or Pacific Ocean temperatures (e.g. Castro et al. 2001). The actual sources of predictability in the CORE subregion have not been demonstrated convincingly but we suggest that additional research is warranted on this topic. The NAME Forecast Forum (Gochis et al. 2009), launched since the NAME field campaign, could serve as a useful platform for such studies.

Second, prediction of the onset of monsoon precipitation is likely to be difficult considering the sometimes-ambiguous observational start of the 'rainy season'. We used precipitation as the basis for defining onset in this study (Table 3), and the assessment of monsoon onset in section 3a indicated some of the arbitrariness in defining onset (as shown in Fig. 5). Some investigators in the U.S., including U.S. National Weather Service forecast offices in Arizona, prefer to use humidity as a smoother, less transient indicator of the onset of the 'wet' season (Ellis et al. 2004). As a complement to additional research on seasonal predictability in the CORE subregion, the definition of 'monsoon onset' itself in the U.S. and Mexico requires additional investigation.

The NAMAP and NAMAP2 modeling exercises grew out of a desire to integrate model assessment and development more closely into a well-defined field measurement campaign. We have not attempted to conduct a truly comprehensive development effort on multiple models, and many active monsoon simulation efforts are being carried out independently of the NAMAP projects. Despite its limitations, NAMAP2 seems to confirm that model simulations of the characteristic features of the monsoon are improving, suggesting that the scope of sensitivity

studies can reasonably be extended beyond simply assessing whether models are capable of generating fairly realistic results on the monthly and seasonal time scale.

One of the key outcomes of the NAMAP2 exercise is that it serves to highlight uncertainties in *both* models and observations. The NAME project has taken place in a data sparse region with complex mesoscale features that pose special challenges for both numerical models and data analysis algorithms. Improvements in simulation and observational capability need to proceed in parallel to facilitate the improvements in prediction that are the ultimate goal of NAME.

5. Conclusions

NAMAP2 involved ten atmospheric modeling groups (6 global, 4 regional) which carried out a coordinated set of simulations of the 2004 North American monsoon season. Each simulation was forced by observed, time-varying ocean temperatures; in addition, the regional models used observed, time-varying lateral atmospheric boundary conditions. Modeling metrics developed in the previous NAMAP assessment were used to provide structure to the NAMAP2 analysis described in this article. A much more complete set of NAMAP2 graphics is freely available in an online atlas.

All models examined in this study achieved some degree of fidelity in simulating the onset and seasonal evolution of the monsoon and the diurnal cycle of precipitation, but, as expected, there were considerable differences among models in the simulations. Despite these differences, the general success of the models in generating a summer rainfall maximum in the NAM domain represents a significant advance over pre-NAME modeling efforts, and suggests that more focused dynamical prediction and model sensitivity efforts are well worth pursuing.

Several specific processes have been identified that represent targets for model development efforts. The transition from convective to resolved precipitation presents a difficult challenge for the models, especially so for high resolution models with grid cells sufficiently small to generate resolved ascent following the initiation of afternoon subgrid-scale moist convection. The degree of coupling of precipitation and surface fluxes varies widely from model to model. The role of a

climatological low-level jet in the Gulf of California for successful monsoon simulation remains somewhat unclear.

For some of these processes (such as the fluxes associated with land surface variables), and indeed any process involving precipitation, validating the model results using the observational data base remains difficult. In this regard, NAMAP2 can be considered a test of data quality as much as an assessment of model fidelity. The uncertainties in precipitation analyses presented herein illustrate this point. Advances and improvements in modeling and observations should proceed in parallel, working toward the overarching long-term goal of NAME: to leave a legacy of improved observations, process-based understanding, simulation capability, and ultimately prediction skill for summer climate variability associated with the North American monsoon.

Acknowledgements. Support for analysis of the NAMAP2 output at UNM and CPC, and for the NAMAP2 online atlas at U. Miami, was derived from a grant from the NOAA Climate Prediction Program for the Americas. The UCAR Joint Office for Science Support created and maintained the NAMAP2 web page as part of overall NAME web support. We thank Dr. David Gochis for providing NERN rainfall data. Dr. Gochis and two anonymous referees provided very constructive manuscript reviews.

REFERENCES

Anderson, B.T., J.O. Roads, S.-C. Chen, and H-M.H. Juang, 2000: Regional simulation of the low-level monsoon winds over the Gulf of California and southwestern United States. *J. Geophys. Res.*, **105**, 17,955-17,969.

——, ——, —— and ——, 2001: Model dynamics of summertime low-level jets over northwestern Mexico. *J. Geophys. Res.*, **106**, 3401-3413.

Anthes, R.A., E.Y. Hsie and Y.H. Kuo, 1987: *Description of the PSU/NCAR mesoscale model version 4 (MM4).* NCAR Technical Note, NCAR/tn 282+STR, 66 pp.

Arritt, R.W., D.C. Goering, and C.J. Anderson, 2000: The North American Monsoon system in the Hadley Centre coupled ocean-atmosphere GCM. *Geophys. Res. Lett.*, **27**, 565-568.

Berbery, E.H., 2001: Mesoscale moisture analysis of the North American Monsoon. *J. Climate,* **14**, 121-137.

Campana, K., and P. Caplan, Eds., 2005: Technical Procedure Bulletin for T382 Global Forecast System. Available online at `http://www.emc.ncep.noaa.gov/gc_wmb/Documentation/TPBoct05/T382.TPB.FINAL.htm`

Castro, C.L., T.B. McKee, and R.A. Pielke Jr., 2001: The relationship of the North American Monsoon to tropical and North Pacific sea surface temperatures as revealed by observational analyses. *J.Climate*, **14**, 4449-4473.

Collier, J. C., and G. J. Zhang, 2006: Simulation of the North American Monsoon by the NCAR CCM3 and its sensitivity to convection parameterization. *J. Climate*, **19**, 2851–2866.

——, and ——, 2007: Effects of increased horizontal resolution on simulation of the North American Monsoon in the NCAR CAM3: An evaluation based on surface, satellite, and reanalysis data. *J. Climate*, **20**, 1843-1861.

Collins, W.D., P.J. Rasch, B.A. Boville, J.J. Hack, J.R. McCaa, D.L. Williamson, B.P. Briegleb, C.M. Bitz, S.-J. Lin and M. Zhang, 2006: The formulation and atmospheric simulation of the Community Atmosphere Model: CAM3. *J. Climate,* **19**, 2144–2161.

Ellis, A.W., E.M. Saffell, and T.W. Hawkins, 2004: A method for defining monsoon onset and demise in the southwestern USA. *Int. J. Climatol.*, **24**, 247-265.

Fawcett, P.J., J.R. Stalker and D.S. Gutzler, 2002: Multistage moisture transport into the interior of northern Mexico during the North American summer monsoon. *Geophys. Res. Lett.*, **29**, doi:10.1029/2002GL015693.

Gochis, D.J., W.J. Shuttleworth and Z.-L. Yang, 2002: Sensitivity of the modelled North American Monsoon regional climate to convective parameterization. *Mon. Wea. Rev.*, **130**, 1282–1298.

——, —— and ——, 2003: Hydrometeorological response of the modeled North American Monsoon to convective parameterization. *J. Hydrometeor.*, **4**, 235–250.

——, C.J. Watts, J. Garatuza-Payan and J. Cesar-Rodriguez, 2007: Spatial and temporal patterns of precipitation intensity as observed by the NAME event rain gauge network from 2002 to 2004. *J. Climate*, **20**, 1734-1750.

——, J. Schemm, W. Shi, L. Long, W. Higgins and A. Douglas, 2009: A forum for evaluating forecasts of the North American Monsoon. *EOS, Transactions Amer. Geophys. Union*, **29**, 249-250.

——, S. Nesbitt, W. Yu and S.F. Willams, 2009: Assessment of quantitative precipitation estimates from space-borne platforms during the 2004 North American Monsoon Experiment. *Atmósfera*, **22**, 69-98.

Gutzler, D.S., 2000: Covariability of spring snowpack and summer rainfall across the Southwest United States. *J. Climate*, **13**, 4018-4027.

——, 2004: An index of interannual precipitation variability in the core of the North American monsoon region. *J. Climate,* **17,** 4473–4480.

——, H.-K. Kim, R.W. Higgins, H. Juang, M. Kanamitsu, K. Mitchell, K.C. Mo, P. Pegion, E.A. Ritchie, J.-K. Schemm, S.D. Schubert, Y. Song and R. Yang,, 2004: North American monsoon Model Assesment Project (NAMAP). NCEP/ Climate Prediction Center ATLAS No. 11, 32 pp. [Available from NOAA Climate Prediction Center, 5200 Auth Road, Camp Springs, MD 20746 and online at `http://www.cpc.ncep.noaa.gov/research_papers/ncep_cpc_atlas/11/atlas11.htm`]

——, ——, ——, ——, ——, ——,——, ——, ——, ——, ——, —— and ——, 2005: The North American Monsoon Model Assessment Project: Integrating numerical modeling into a field-based process study. *Bull. Amer. Meteor. Soc.*, **86**, 1423-1429.

Higgins, R.W., Y. Yao, and X. Wang, 1997: Influence of the North American Monsoon system on the United States summer precipitation regime. *J. Climate*, **10**, 2600-2622.

——, W. Shi, E. Yarosh and R. Joyce, 2000: *Improved United States Precipitation Quality Control System and Analysis.* NCEP/Climate Prediction Center ATLAS No. 7, 40 pp. [Available from NOAA Climate Prediction Center, 5200 Auth Road, Camp Springs, MD 20746]

——, W. Shi and C. Hain, 2004: Relationships between Gulf of California moisture surges and precipitation in the southwestern United States. *J. Climate,* **17***,* 2983-2997.

——, J. Amador, A. Barros, E.H. Berbery, E. Caetano, R. Cifelli, R. Carbone, M. Cortez-Vazquez, A.V. Douglas, M.W. Douglas, G. Emmanuel, D.J. Gochis, D. Gutzler, R. Johnson, C. King, D.

Lettenmaier, T. Lang, R. Lobato, R. Maddox, V. Magaña, J. Meitin, K.C. Mo, E. Pytlak, C. Ropelewski, S. Rutledge, J. Schemm, S.D. Schubert, F. Torres, A. White, C. Williams, A. Wood, R. Zamora and C. Zhang, 2006: The North American Monsoon Experiment field campaign and modeling strategy. *Bull. Amer. Meteor. Soc.*, **87**, 79-94.

Huffman, G.J., R.F. Adler, D.T. Bolvin, G.Gu, E.J. Nelkin, K.P. Bowman, Y. Hong, E.F. Stocker, and D.B. Wolff, 2007: The TRMM Multi-satellite Precipitation Analysis (TMPA): Quasi-global, multi-year, combined-sensor precipitation at fine scales. *J. Hydrometeor.*, **8**, 38-55.

Janowiak, J.E., V.J. Dagostaro, V.E. Kousky and R.J. Joyce, 2007: An examination of precipitation in observations and model forecasts during NAME with emphasis on the diurnal cycle. *J. Climate*, **20**, 1680-1692.

Johnson, R.H., P.E. Ciesielski, B.D. McNoldy, P.J. Rogers, and R.K. Taft, 2007: Multiscale variability of the flow during the North American Monsoon Experiment. *J. Climate*, **20**, 1628–1648.

Juang, H.M.H., and M. Kanamitsu, 1994: The NMC nested regional spectral model. *Mon. Wea. Rev.,* **122***,* 3-26.

Kanamitsu, M., W. Ebisuzaki, J. Woolen, S. K. Yang, J. J. Hnilo, M. Fiorina and G. L. Potter, 2002: NCEP/DOE AMIP-II reanalysis (R-2). *Bull Amer. Meteor. Soc.,* **83**, 1631-1643.

——, and K.C. Mo, 2003: Dynamical effect of land surface processes on summer precipitation over the southwestern United States. *J. Climate*, **16**, 496-509.

Kelly, P., and B. Mapes, 2009: Land surface heating and the North American Monsoon: Model evaluation from diurnal to seasonal. *J. Climate*, submitted for publication [reference to be updated at proof stage].

Lawrence, D.M., P.E. Thornton, K.W. Oleson and G.B. Bonan, 2007: The partitioning of evapo-transpiration into transpiration, soil evaporation, and canopy evaporation in a GCM: Impacts on land–atmosphere interaction. *J. Hydrometeor.*, **8**, 862–880.

Lee, M., S. Schubert, M. Suarez, I. Held, A. Kumar, T.L. Bell, J.E. Schemm, N. Lau, J.J. Ploshay, H. Kim and S.-H. Yoo, 2007a: Sensitivity to horizontal resolution in the AGCM simulations of warm season diurnal cycle of precipitation over the United States and northern Mexico. *J. Climate*, **20**, 1862-1881.

——, ——, ——, ——, N. Lau, J. Ploshay, A. Kumar, H. Kim and J. Schemm, 2007b: An analysis of the warm season diurnal cycle over the continental United States and northern Mexico in general circulation models, *J. Hydrometeor.*, **8**, 344-366.

——, ——, ——, J. Schemm, H. Pan, J. Han and S. Yoo, 2008: The role of convection triggers in the simulation of the diurnal cycle of precipitation over the United States Great Plains in a general circulation model. *J. Geophys. Res.*, **113**, D02111, doi:10.1029/2007JD008984.

Lin, J.-L., B.E. Mapes, K.M. Weickmann, G.E. Kiladis, S.D. Schubert, M.J. Suarez, J.T. Bacmeister and M.-I. Lee, 2008: North American Monsoon and convectively coupled equatorial waves simulated by IPCC AR4 coupled GCMs. *J. Climate*, **21**, 2919-2937.

Lin, S.J., 2004: A "Vertically Lagrangian" finite-volume dynamical core for global models. *Mon. Wea. Rev.*, **132**, 2293–2307.

Mesinger, F., G. DiMego, E. Kalnay, K. Mitchell, P.C. Shafran, W. Ebisuzaki, D. Jović, J. Woollen, E. Rogers, E.H. Berbery, M. Ek, Y. Fan, R. Grumbine, W. Higgins, H. Li, Y. Lin, G. Manikin, D. Parrish and W. Shi, 2006: North American Regional Reanalysis. *Bull. Amer. Meteor. Soc.,* **87**, 343–360.

Mitchell, D.L., D. Ivanova, R. Rabin, T.J. Brown and K. Redmond, 2002: Gulf of California sea surface temperatures and the North American Monsoon: Mechanistic implications from observations. *J. Climate*, **15**, 2261-2281.

Mo, K.C., and H.M.H. Juang, 2003: Influence of sea surface temperature anomalies in the Gulf of California on North American Monsoon rainfall. *J. Geophys. Res.,* **108**, doi:10.1029/2002JD002403.

NAME Science Working Group, 2004: A Science and Implementation Plan for a North American Monsoon Experiment (NAME). [Available from NOAA Climate Prediction Center, 5200 Auth Rd, Camp Springs, MD, 20746 and on the NAME webpage at http://www.eol.ucar.edu/name]

Pielke, R.A., W.R. Cotton, R.L. Walko, C.J. Tremback, W.A. Lyons, L.D. Grasso, M.E. Nicholls, M.D. Moran, D.A. Wesley, T.J. Lee, and J.H. Copeland, 1992: A comprehensive meteorological modeling system--RAMS. *Meteor. Atmos. Phys.*, **49**, 69-91.

Rienecker, M.M., M.J. Suarez, R. Todling, J. Bacmeister, L. Takacs, H.-C. Liu, W. Gu, M. Sienkiewicz, R.D. Koster, R. Gelaro, I. Stajner, and J.E. Nielsen, 2008: The GEOS-5 Data Assimilation System - Documentation of Versions 5.0.1, 5.1.0, and 5.2.0. Technical Report Series on Global Modeling and Data Assimilation, **27**, 101 pp, available online at

`http://gmao.gsfc.nasa.gov/pubs/docs/Rienecker369.pdf`

Saha, S., S. Nadiga, C. Thiaw, J. Wang, W. Wang, Q. Zhang, H.M. van den Dool, H.-L. Pan, S. Moorthi, D. Behringer, D. Stokes, M. Pena, S. Lord, G. White, W. Ebisuzaki, P. Peng and P. Xie, 2006: The NCEP Climate Forecast System. *J. Climate,* **19**, 3483–3517

Saleeby, S.M., and W.R. Cotton, 2004: Simulations of the North American Monsoon system. Part I: Model analysis of the 1993 monsoon season. *J. Climate*, **17**, 1997–2018.

Small, E.E., 2001: The influence of soil moisture anomalies on variability of the North American Monsoon system. *Geophys. Res. Lett.,* **28**, 139-142.

Stensrud, D.J., R.L. Gall, S.L. Mullen and K.W. Howard, 1995: Model climatology of the Mexican Monsoon. *J. Climate*, **8**, 1775-1794.

——, ——, and M.K. Nordquist, 1997: Surges over the Gulf of California during the Mexican monsoon. *Mon. Weather Rev.,* **125**, 417-436.

Vivoni, E.R., H.A. Moreno, G. Mascaro, J.C. Rodriguez, C.J. Watts, J. Garatuza-Payan and R.L. Scott, 2008: Observed relation between evapotranspiration and soil moisture in the North American monsoon region. *Geophys. Res. Lett.*, **35**, L22403, doi:10.1029/ 2008GL036001.

Wang, W., and P. Xie, 2007: A multiplatform-merged (MPM) SST analysis. *J. Climate*, **20**, 1662-1679.

Watts, C.J., R.L. Scott, J. Garatuza-Payan, J.C. Rodriguez, J.H. Prueger, W.P. Kustas and M. Douglas, 2007: Changes in vegetation condition and surface fluxes during NAME 2004. *J. Climate*, **20**, 1810–1820.

Williams, C.R., A.B. White, K.S. Gage, and F.M. Ralph, 2007: Vertical structure of precipitation and related microphysics observed by NOAA profilers and TRMM during NAME 2004. *J. Climate*, **20**, 1693–1712.

Xu, J., and E.E. Small, 2002: Simulating summertime rainfall variability in the North American Monsoon region: The influence of convection and radiation parameterizations. *J. Geophys. Res.*, **107**, doi:10.1029/2001JD002047.

Yang, Z.-L., D. Gochis, and W.J. Shuttleworth, 2001: Evaluation of the simulations of the North American Monsoon in the NCAR CCM3. *Geophys. Res. Lett.*, **28**, 1211-1214.

APPENDIX. LIST OF ACRONYMS

AGCM	Atmospheric General Circulation Model
AMIP	Atmospheric Model Intercomparison Project
AZNM	Arizona / New Mexico Region
CAM3	Community Atmosphere Model, Version 3
CFS	Climate Forecast System
FVM	Finite Volume Model
GEOS-5	Goddard Earth Observing System, Version 5
GFDL	NOAA Geophysical Fluid Dynamics Laboratory
GFS	Global Forecast System
LLJ	Low Level Jet
MM5	Fifth-Generation NCAR / Penn State Mesoscale Model
MPM SST	Multi Platform Merged Sea Surface Temperature
NAME	North American Monsoon Experiment
NAMAP2	North American Monsoon Model Assessment Project 2
NARR	North American Regional Reanalysis
NASA	National Aeronautics and Space Administration
NCAR	National Center for Atmospheric Research
NCEP	National Centers for Environmental Prediction
NERN	NAME Event Rain gauge Network
NOAA	National Oceanic and Atmospheric Administration
RAMS	Regional Atmospheric Modeling System
RMORPH	Research version of CPC's Rainfall Morphing Technique (CMORPH)
RSM	Regional Spectral Model
TRMM	Tropical Rainfall Measuring Mission
URD	Unified Rainfall Dataset

Table 1. Table of boundary conditions used in the NAMAP2 simulations.

Simulation Period	15 May-30 Sept 2004
Computational Domain	15-45°N 125-75°W
Lateral Boundary Conditions (for regional models)	NOAA CDAS2
Surface Boundary Conditions (ocean)	MPM analysis (Wang and Xie 2007)
Surface Boundary Conditions (land)	chosen by each modeling group

Table 2. Models participating in NAMAP2 and their key characteristics. The six global models are indicated in non-italic type; four regional models in italics.

Model Name	Affiliation / Contact	Reference	Horizontal Resolution	Vertical Levels	Ensemble Size	SST Prescription
CFS (Operational)	NOAA CPC / Schemm	Saha et al. (2006)	T126 (~1°)	64	5	MPM
GFS	NOAA CPC / Mo & Wei	Campana et al. (2005)	T126	64	4	MPM
CAM3_a	UCSD SIO / Collier & Zhang	Collins et al. (2006)	T42 (~2.8°)	26	1	Era-40
CAM3_b	NCAR / Lawrence	Collins et al. (2006)	1.0°×1.25°	26	1	Hadley
CAM3_c	UCSD SIO / Collier & Zhang	Collins et al. (2006)	T42 (~2.8°)	26	3	MPM
Finite Volume	NASA GSFC / Bosilovich	Lin (2004)	0.25°×0.36°	32	2	MPM
GEOS5	NASA GSFC / Lee & Schubert	Rienecker et al. (2008)	0.5°×0.67°	72	5	MPM
RAMS	*Duke U / Roy*	*Pielke et al. (1992)*	*64 km*	*30*	*1*	*NOAA OI*
RSM	*UCSD SIO / Nunes & Roads*	*Juang and Kanamitsu (1994)*	*30 km*	*28*	*1*	*MPM*
MM5_a	*IMTA / Lobato*	*Anthes et al. (1987)*	*30 km*	*23*	*3*	*MPM*
MM5_b	*UNM / Ritchie*	*Anthes et al. (1987)*	*15 km*	*33*	*1*	*MPM*

Table 3. Onset dates for each observation product and model for the AZNM and CORE Subregions.

NAMAP2 2004 Monsoon Onset Dates

Observational Products

	URD	RMORPH	TRMM
CORE	5-Jun	4-Jun	6-Jun
AZNM	11-Jul	11-Jul	26-Jun

Rainfall Threshold

	3 Consecutive Days Over
CORE	1.5 mm/day
AZNM	0.5 mm/day

Global Models

	CAM3a	CAM3b	CAM3c	CFS	FVM	GEOS5	GFS
CORE	10-Aug	1-Jun	14-Jun	5-Jun	1-Jun	9-Jun	29-Jun
AZNM	4-Jun	1-Jun	3-Jun	9-Jun	7-Jun	13-Jun	9-Jul

Regional Models

	MM5a	MM5b	RAMS	RSM
CORE	2-Jun	3-Jun	11-Jul	5-Jun
AZNM	3-Jun	3-Jun	13-Jul	22-Jun

LIST OF FIGURES

1. Three observed estimates of total precipitation during the 4-month NAME Enhanced Observing Period, June-Sept 2004. CORE, AZNM and Tier 1.5 analysis subregions are shown (see text for details). The specified computational domain for regional models is slightly larger than the area plotted here. The NAME Tier 1 region encompasses AZNM and CORE, and some additional surrounding area, in a single averaging box. (a) URD, a gauge-based analysis defined only over land areas (b) RMORPH, a blend of gauge and satellite infrared measurements (c) TRMM, a satellite radar-based product.
2. Time series of total monthly precipitation, May-Sept 2004. URD, RMORPH and TRMM observational estimates are shown as black lines in each panel. Global model simulations are shown as colored lines in the left-hand panels; regional model simulations are shown as colored lines in the right-hand panels. (a) CORE subregion (b) AZNM subregion (c) Tier 1.5 subregion. In panel (a), a fourth observational estimate (NERN) is shown, derived from rain gauge data collected within the CORE subregion during the NAME field campaign (see text for details).
3. Maps of total monthly precipitation for June through Sept 2004 (cm). (a) RMORPH observations (b) Simulated by MM5a (3-member ensemble average) (c) Simulated by CFS (5-member ensemble average)
4. Maps of total monthly precipitation and monthly mean wind vectors at 850 hPa for June through Sept 2004 (cm). (a) NARR assimilated observations (b) Simulated by MM5a (3-member ensemble average) (c) Simulated by CFS (5-member ensemble average)
5. Daily precipitation (cm) in the CORE subregion for global models (left panels) and regional models (right panels) from June 1 – Sept 19, 2004. Observations from URD, RMORPH and TRMM are repeated in black, grey, and brown in each panel. Arrows indicate date of onset for each model. Observed onset date is represented by the black arrows.
6. Like Fig. 5, but for the AZNM subregion.
7. Monthly average diurnal time series of total precipitation rate (mm/hr) in the CORE subregion, calculated separately for the months of June, July and August 2004. RMORPH and TRMM observational estimates are shown as dashed and solid black lines in each panel. Global model results are shown in the top panel, and regional model results are shown in the bottom panel. Time is labeled along the x-axis as UTC.

8. Monthly average diurnal time series of precipitation rate in the CORE subregion as in Fig. 7, but with total simulated precipitation split into convective (left panels) and resolved precipitation (right panels). Units are mm/hr as in Fig. 7; note expanded axis in (b), the resolved precipitation simulated by global models.

9. Diurnal cycle of total precipitation as in Fig. 7, but for the AZNM subregion.

10. Diurnal cycle of convective and resolved precipitation as in Fig. 8, but for the AZNM subregion. Note the much-expanded ordinate in panel (b).

11. Monthly averages of sensible flux (top) and latent flux (bottom), averaged over the CORE subdomain (land data points only).

12. Monthly averages of sensible flux (top) and latent flux (bottom), averaged over the AZNM subdomain.

13. Monthly averages of surface layer soil moisture averaged over the CORE and AZNM subdomains, expressed as percentages of the layer capacity.

14. Diurnal cycle of 2-m air temperature (K) averaged over the CORE and AZNM subdomains.

15. JJA averages of vector wind and total precipitation from: (a) NARR, 925 hPa 12Z (b) NARR, 925 hPa, 00Z (c) CFS, 925 hPa, 12Z (d) CAM3, 850 hPa, 12Z (e) RSM, 850 hPa, 12Z (f) MM5a, 850 hPa, 00Z.

16. Frequency of daily rainfall rates in gridpoints within the CORE subregion, JJA 2004 [mm/d]. The y-axis shows the percentage of days for which daily rainfall at individual grid cells occurs within the range of values indicated underneath each bar. The first bar in each graph represents zero rainfall, and the second bar represents daily rainfall >0 mm but less than 0.1 mm. The next six bars represent ranges of daily rainfall scaled to the maximum daily value in the data, with the scaling the same for each graph.

    a) URD observations b) TRMM observations c) CFS simulation

FIGURE 1

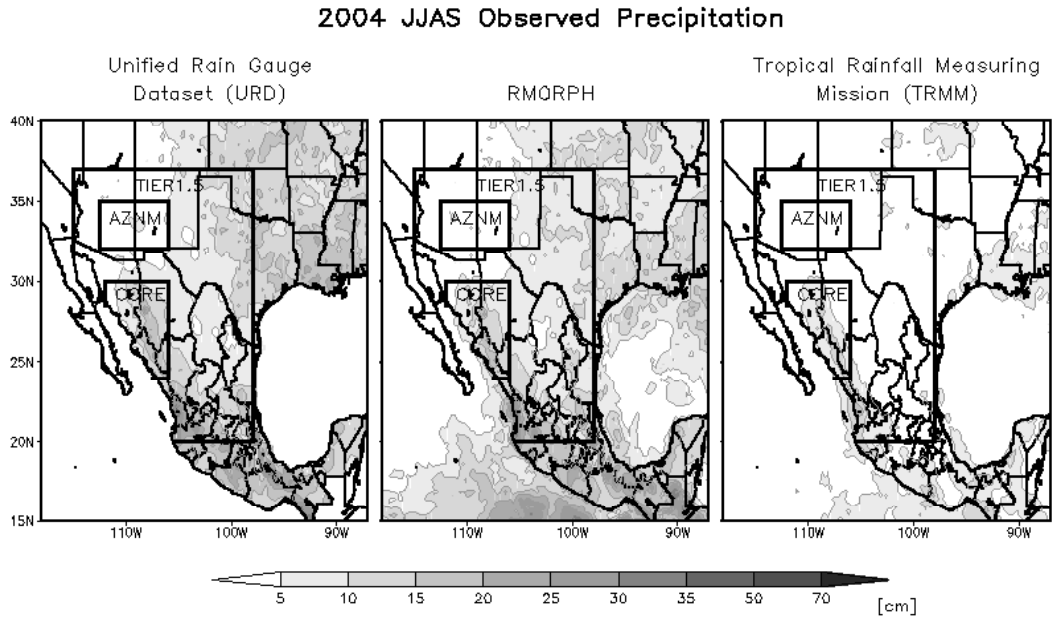

Figure 1. Three observed estimates of total precipitation during the 4-month NAME Enhanced Observing Period, June-Sept 2004. CORE, AZNM and Tier 1.5 analysis subregions are shown (see text for details). The specified computational domain for regional models is slightly larger than the area plotted here. The NAME Tier 1 region encompasses AZNM and CORE (and some additional surrounding area) in a single averaging box. (a) URD, a gauge-based analysis defined only over land areas (b) RMORPH, a blend of gauge and satellite infrared measurements (c) TRMM, a satellite radar-based product.

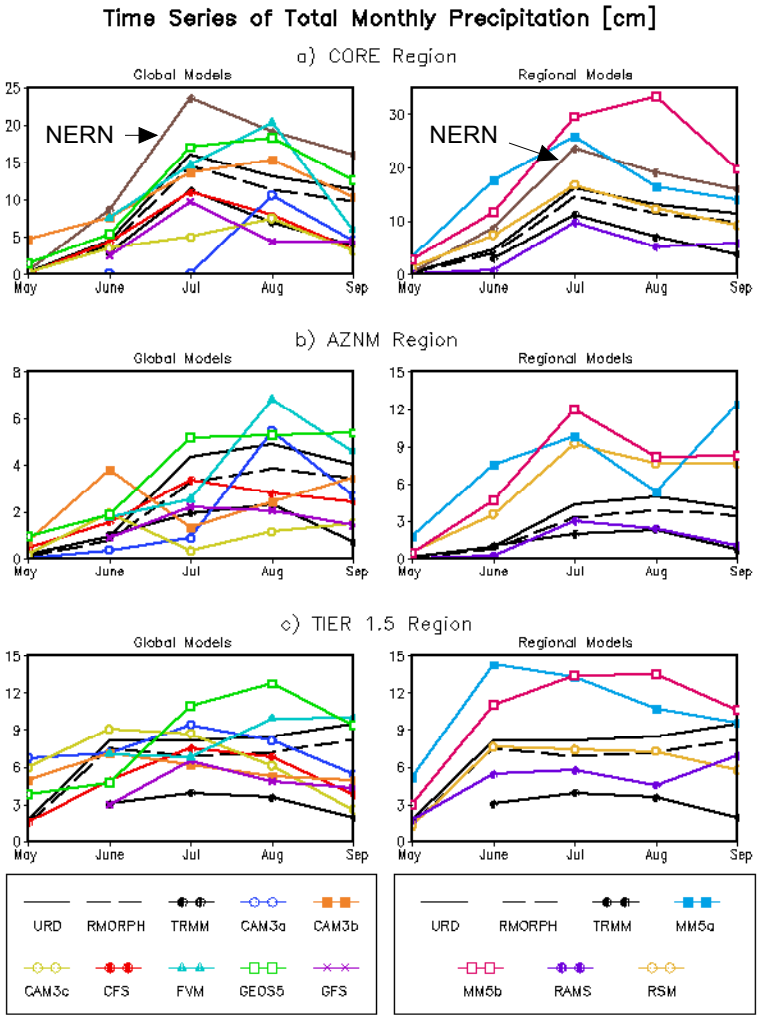

Figure 2. Time series of total monthly precipitation, May-Sept 2004. URD, RMORPH and TRMM observational estimates are shown as black lines in each panel. Global model simulations are shown as colored lines in the left-hand panels; regional model simulations are shown as colored lines in the right-hand panels. (a) CORE subregion (b) AZNM subregion (c) Tier 1.5 subregion. In panel (a), a fourth observational estimate (NERN) is shown, derived from rain gauge data collected within the CORE subregion during the NAME field campaign (see text for details).

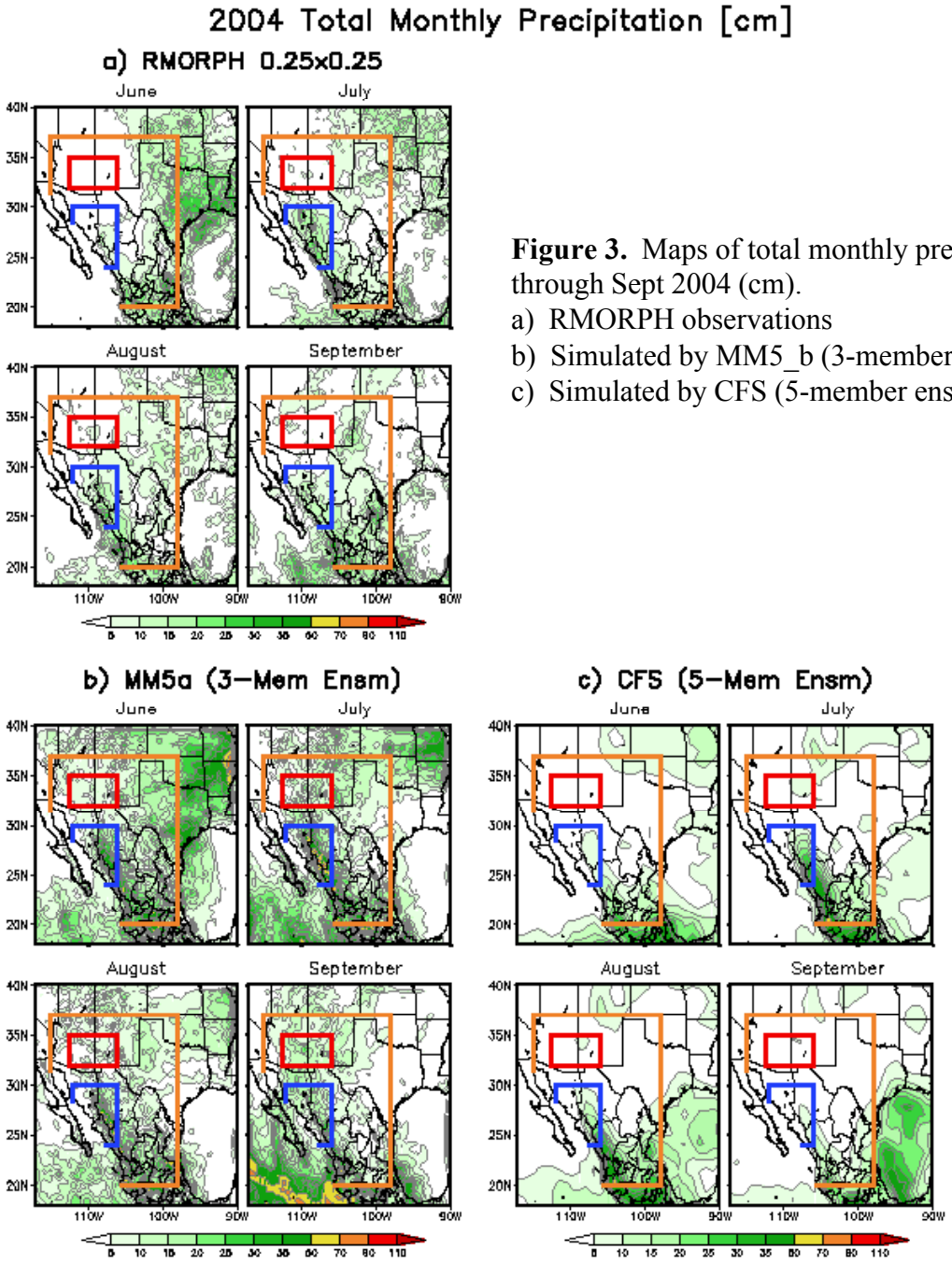

Figure 3. Maps of total monthly precipitation for June through Sept 2004 (cm).

a) RMORPH observations
b) Simulated by MM5_b (3-member ensemble average)
c) Simulated by CFS (5-member ensemble average)

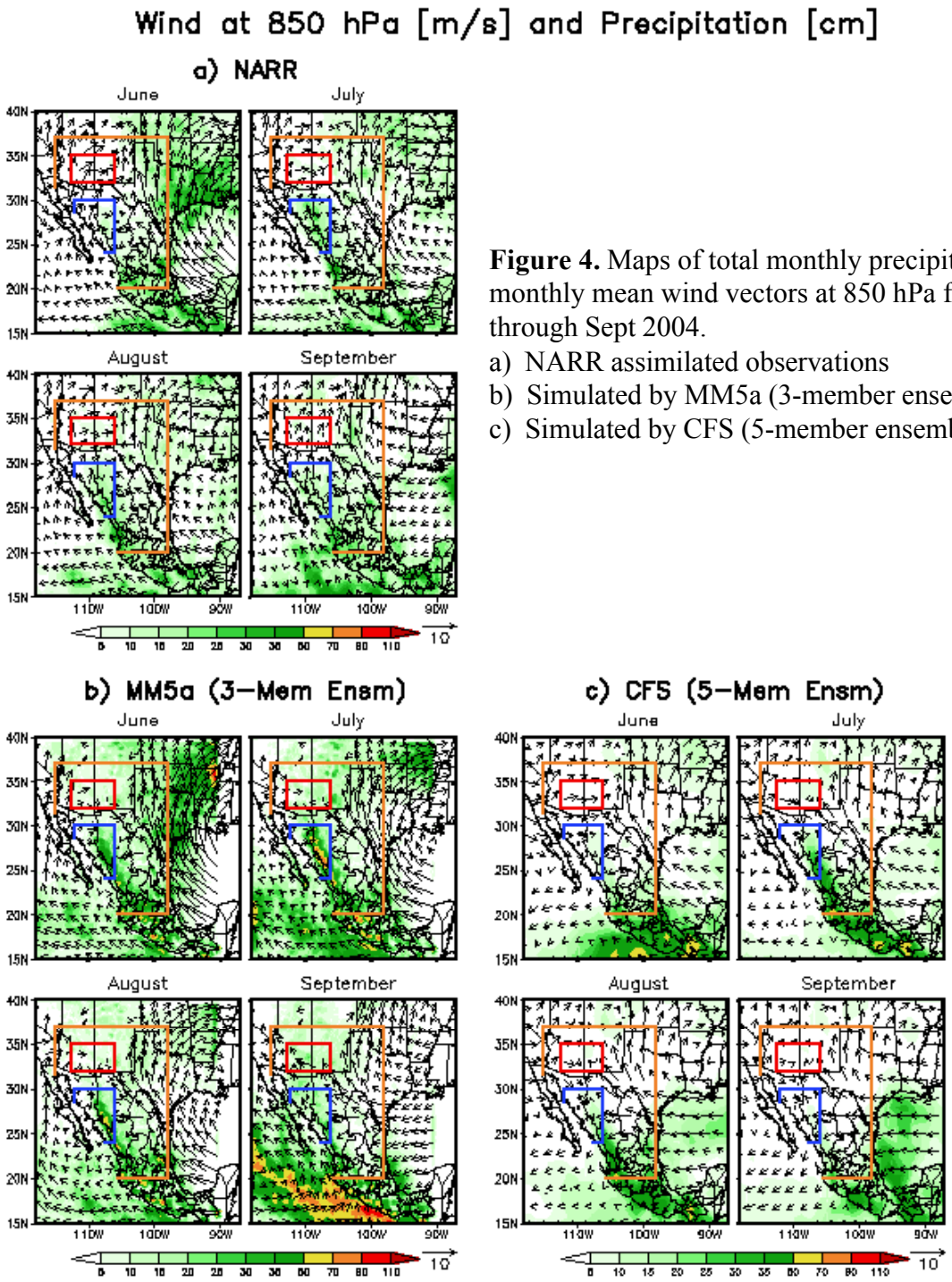

Figure 4. Maps of total monthly precipitation (cm) and monthly mean wind vectors at 850 hPa for June through Sept 2004.

a) NARR assimilated observations
b) Simulated by MM5a (3-member ensemble average)
c) Simulated by CFS (5-member ensemble average)

FIGURE 5

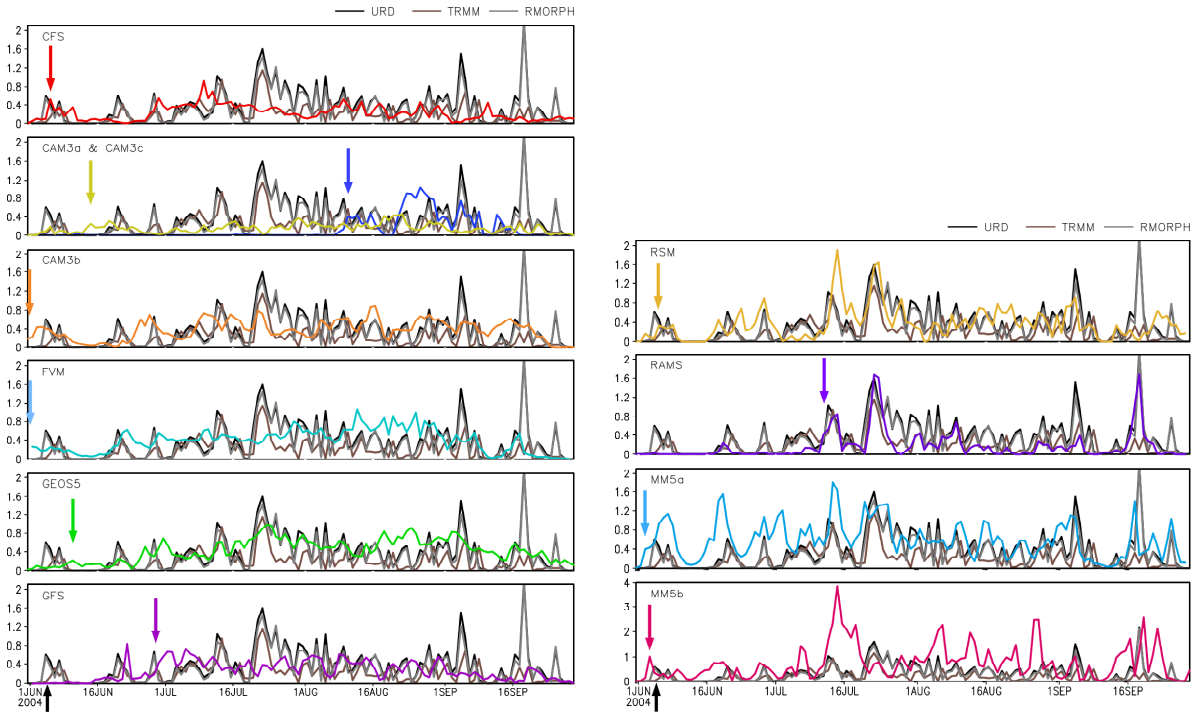

Figure 5. Daily precipitation (cm) in the CORE subregion for global models (left panels) and regional models (right panels) from June 1 – Sept 19, 2004. Observations from URD, RMORPH and TRMM are repeated in black, grey, and brown in each panel.Arrows indicate date of onset for each model. Observed onset date is represented by the black arrows.

Jul 28, 2009

FIGURE 6

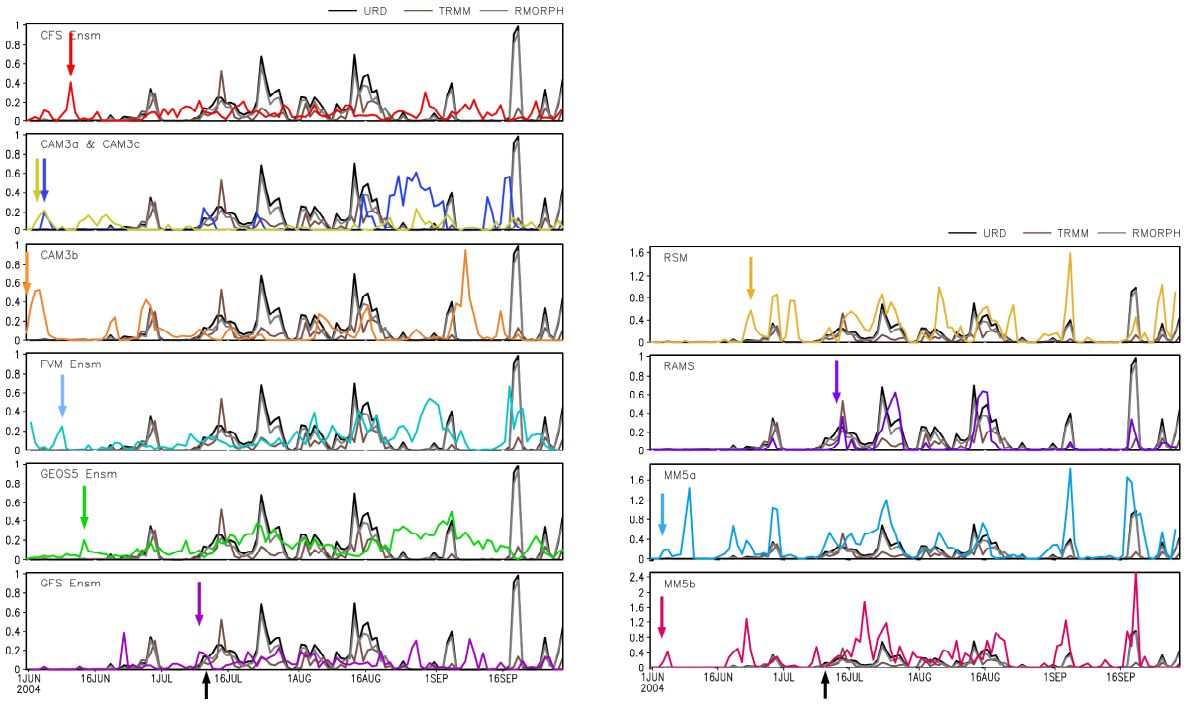

Figure 6. Daily precipitation (cm) in the AZNM subregion for global models (left panels) and regional models (right panels) from June 1 – Sept 19, 2004. Observations from URD, RMORPH and TRMM are repeated in black, grey, and brown in each panel.Arrows indicate date of onset for each model. Observed onset date is represented by the black arrows.

Jul 28, 2009

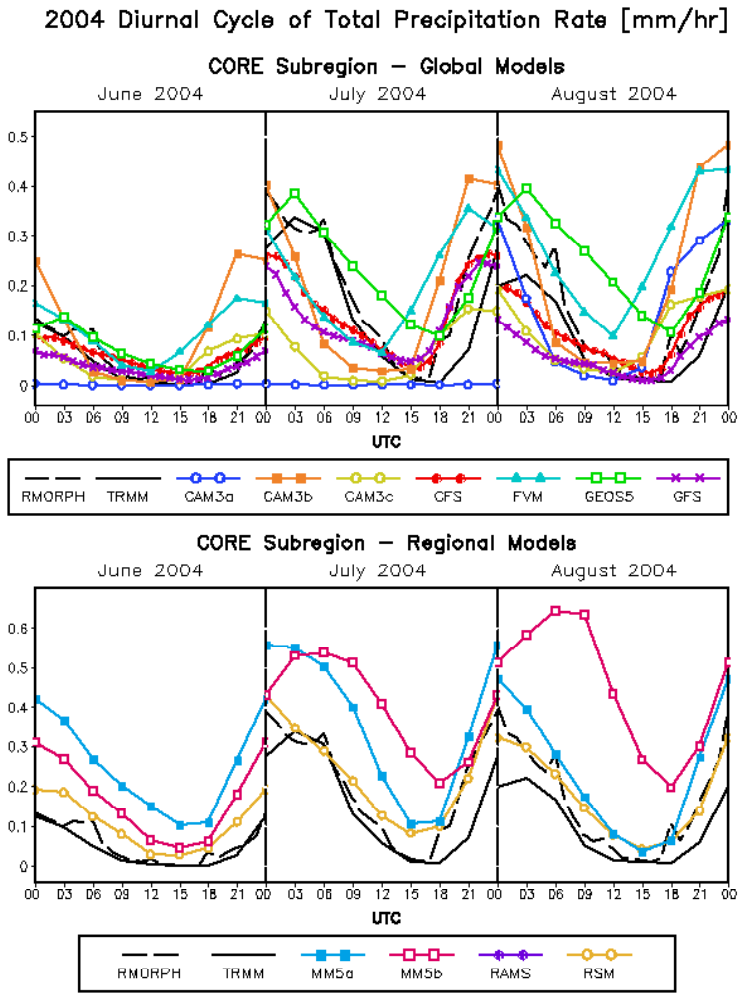

Figure 7. Monthly average diurnal time series of total precipitation rate (mm/hr) in the CORE subregion, calculated separately for the months of June, July and August 2004. RMORPH and TRMM observational estimates are shown as dashed and solid black lines in each panel. Global model results are shown in the top panel, and regional model results are shown in the bottom panel. Time is labelled along the x-axis as UTC.

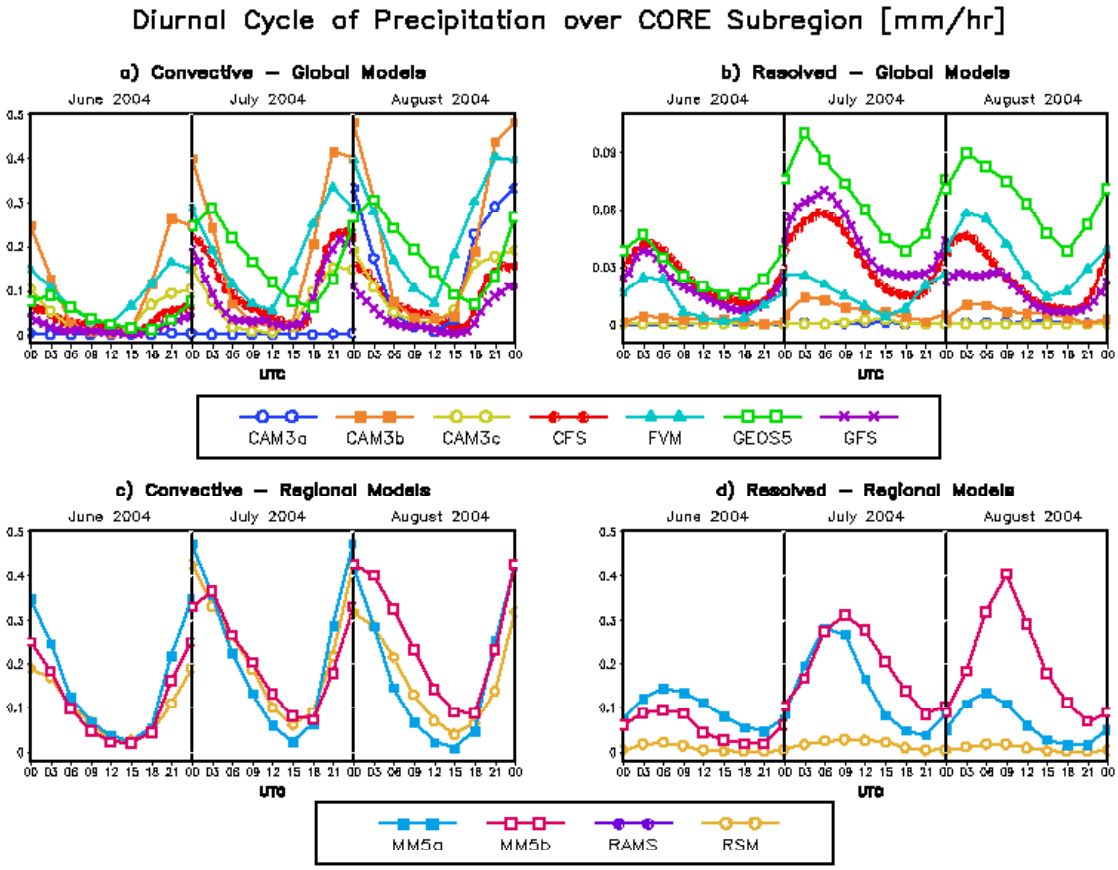

Figure 8. Monthly average diurnal time series of precipitation rate in the CORE subregion as in Fig. 7, but with total simulated precipitation split into convective (left panels) and resolved precipitation (right panels). Units are mm/hr as in Fig. 7; note expanded axis in (b), the resolved precipitation simulated by global models.

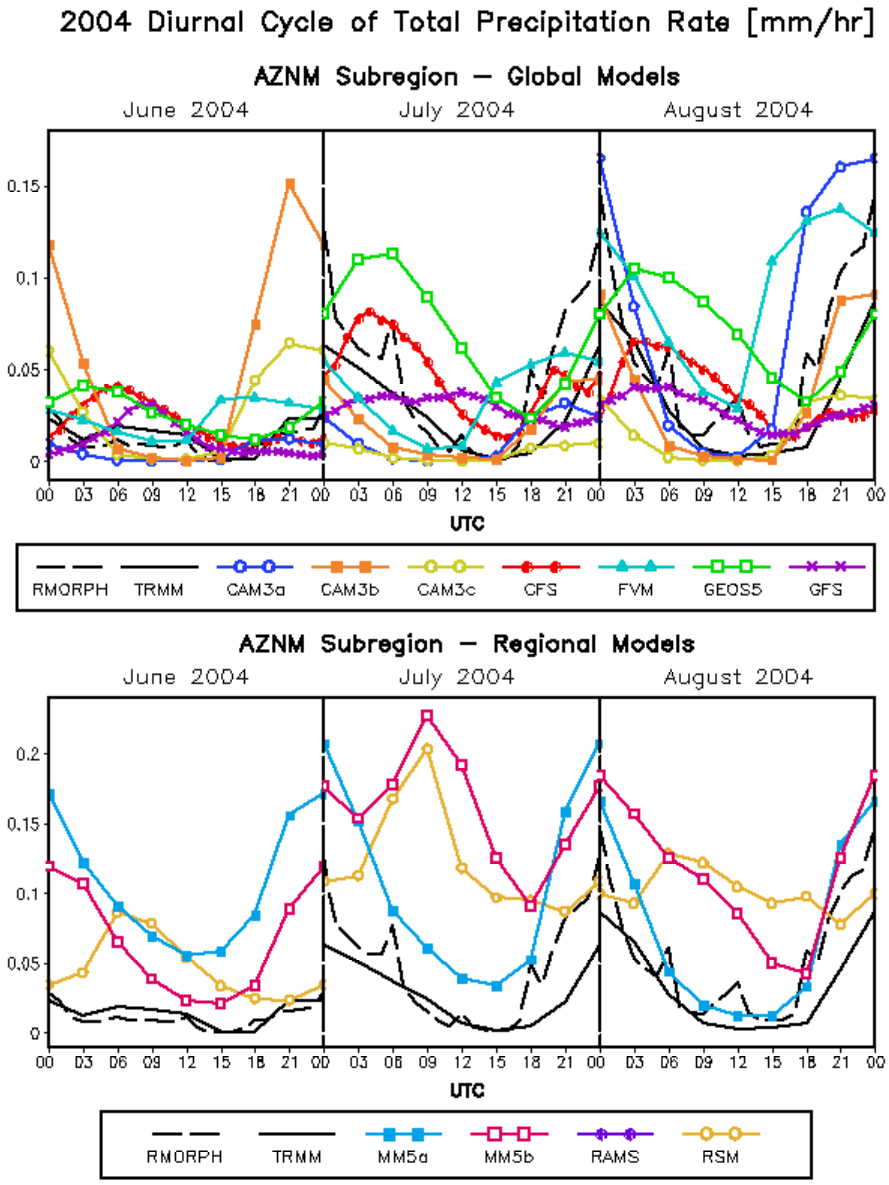

Figure 9. Diurnal cycle of total precipitation as in Fig. 7, but for the AZNM subregion.

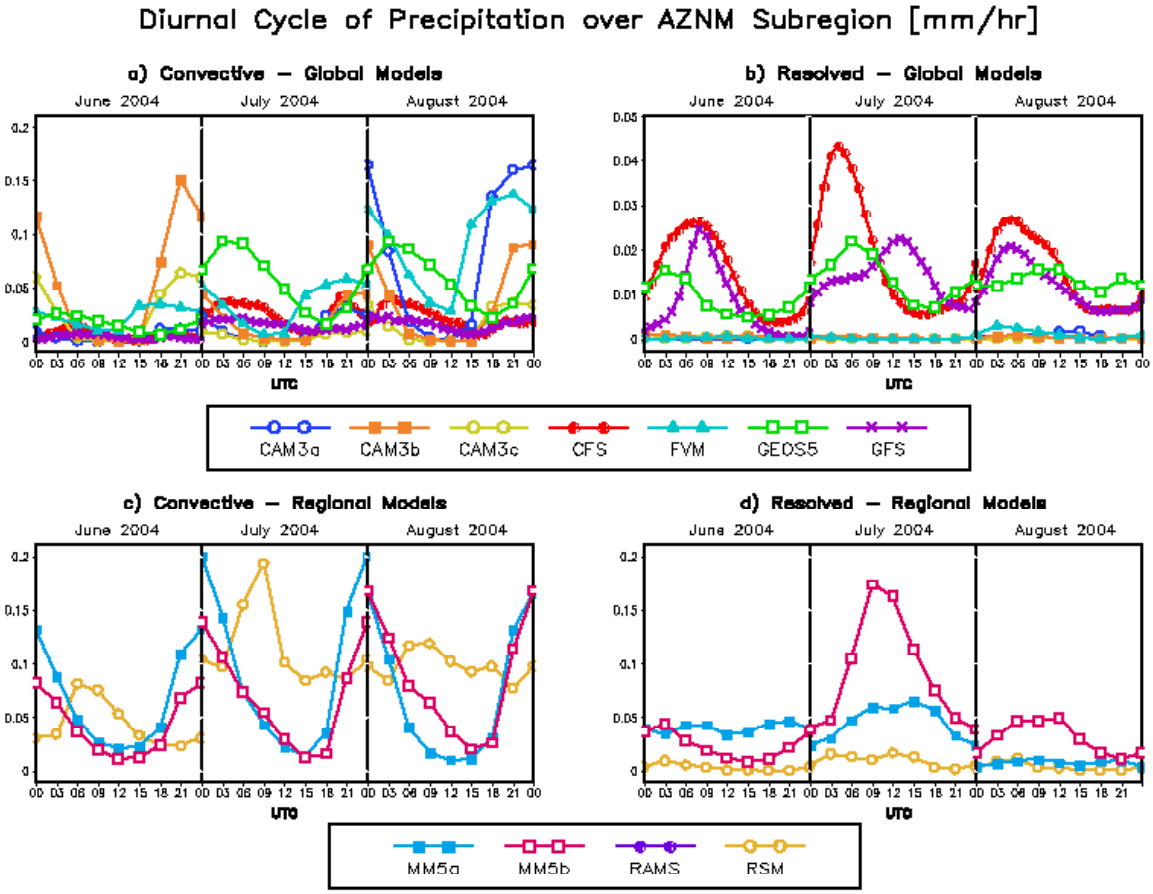

Figure 10. Diurnal cycle of convective and resolved precipitation as in Fig. 8, but for the AZNM subregion. Note the much-expanded ordinate in panel (b).

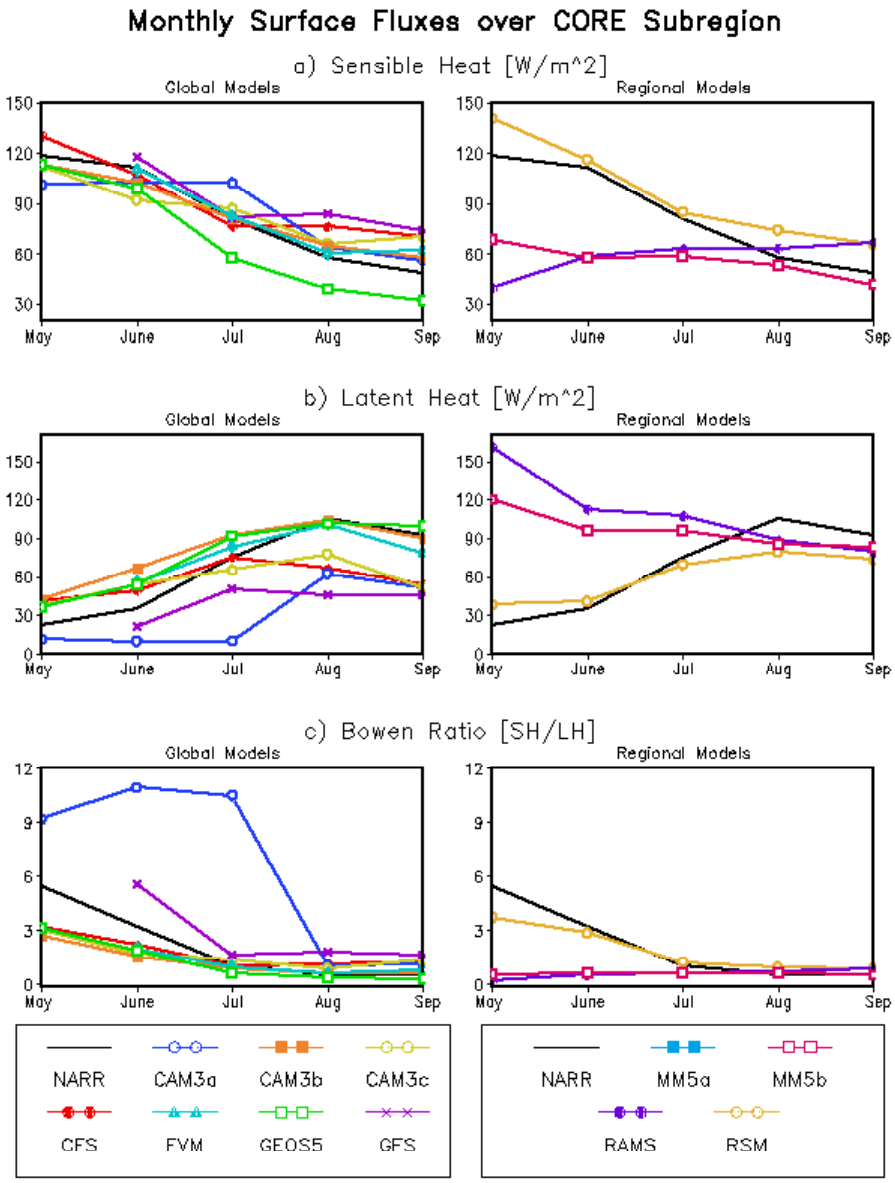

Figure 11. Monthly averages of sensible flux (top) and latent flux (bottom), averaged over the CORE subregion (land data points only).

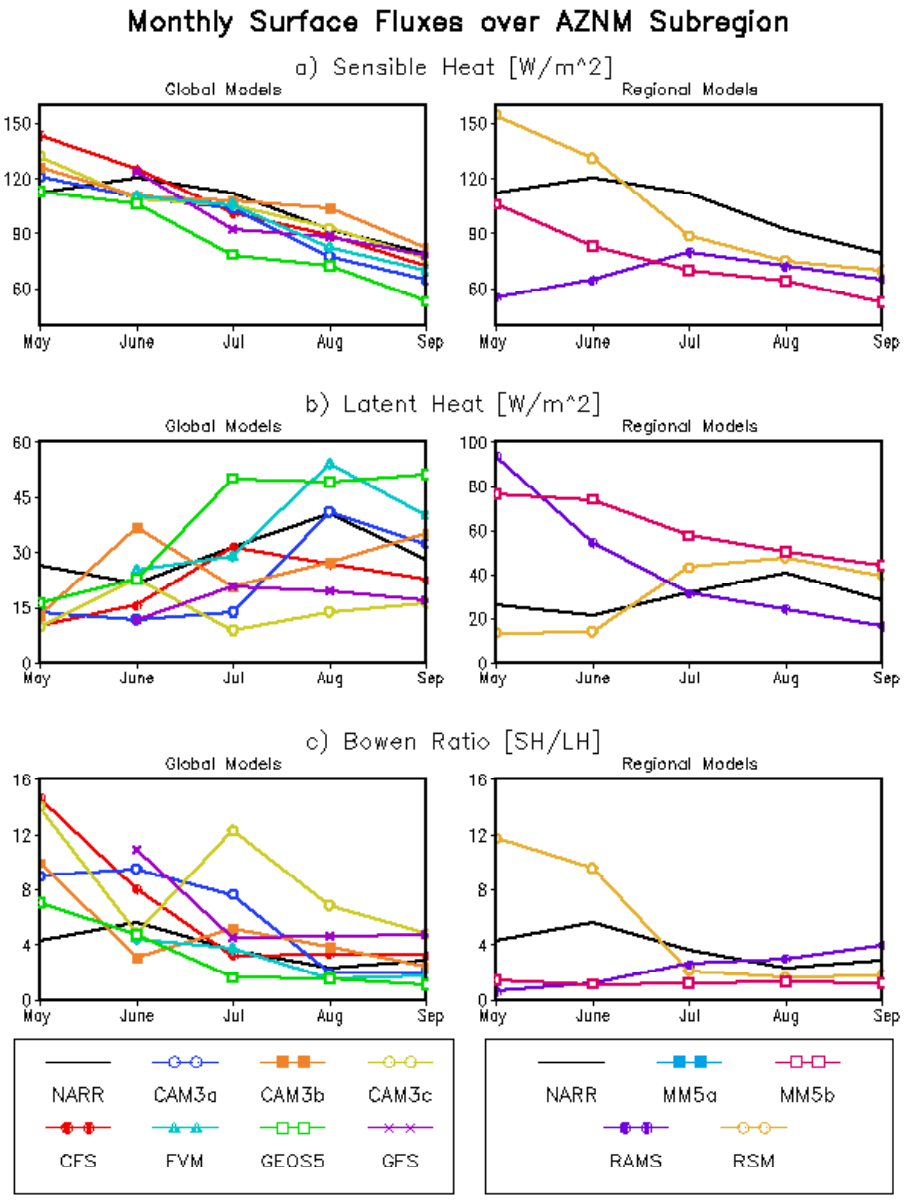

Figure 12. Monthly averages of sensible flux (top) and latent flux (bottom), averaged over the AZNM subregion.

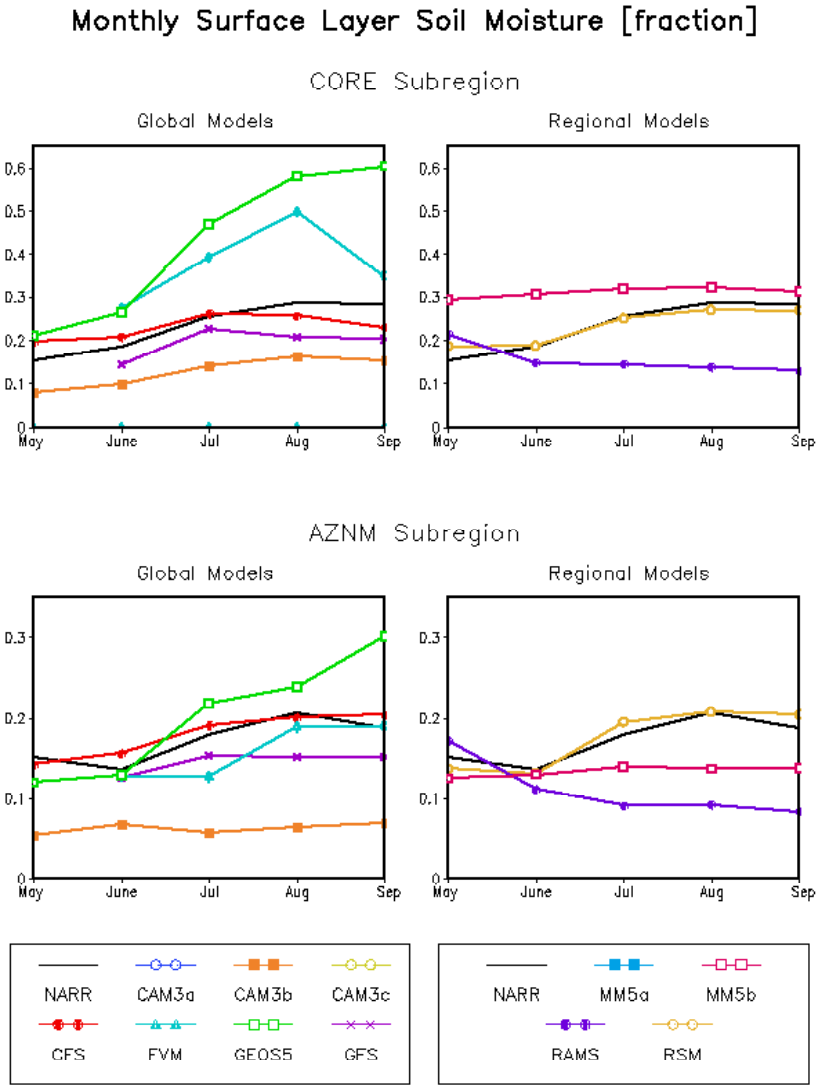

Figure 13. Monthly averages of surface layer soil moisture averaged over the CORE and AZNM subregions, expressed as percentages of the layer capacity.

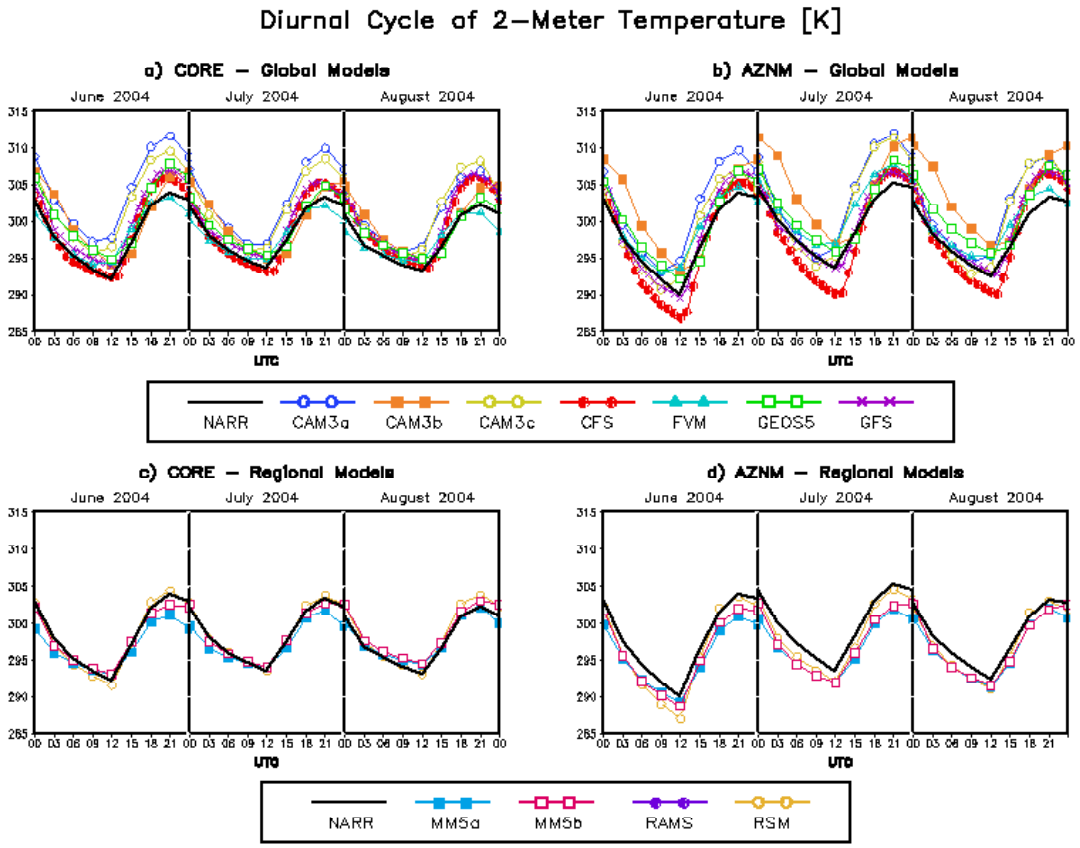

Figure 14. Diurnal cycle of 2-m air temperature (K) averaged over the CORE (left) and AZNM (right) subregions.

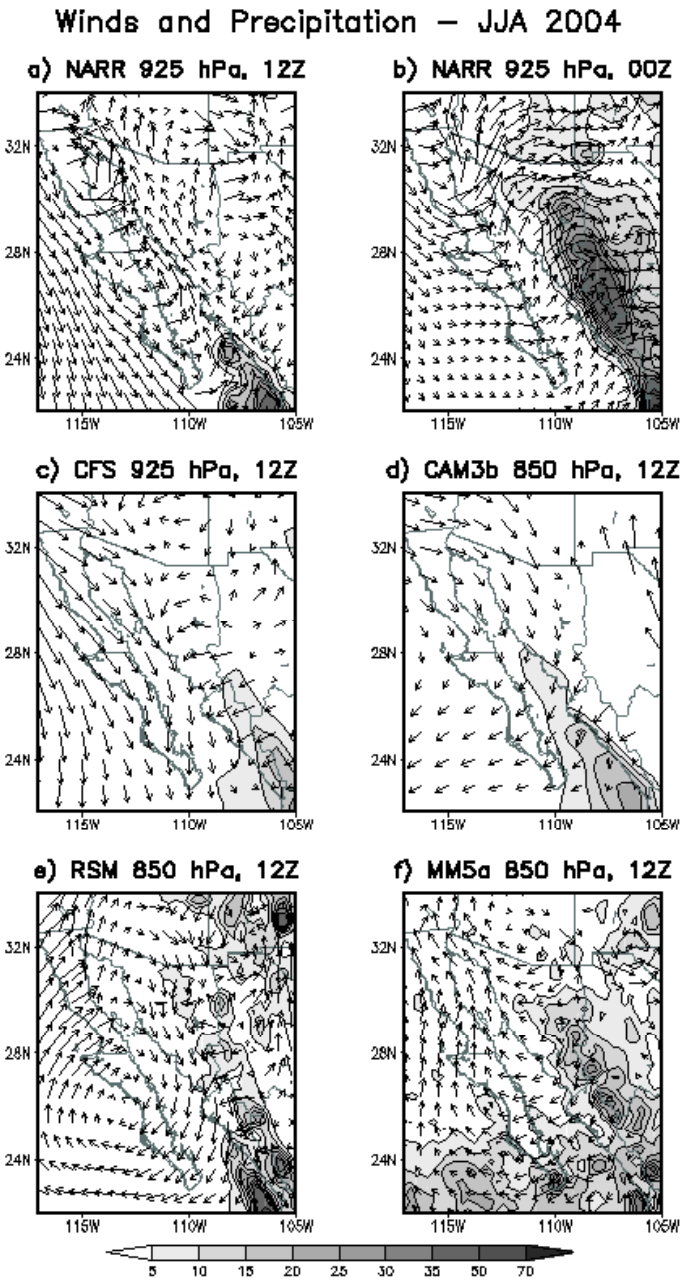

Figure 15. JJA averages of vector wind and total precipitation from: (a) NARR, 925 hPa 12Z (b) NARR, 925 hPa 00Z (c) CFS, 925 hPa 12Z (d) CAM3, 850 hPa, 12Z. (e) RSM, 850 hPa, 12Z (f) MM5a, 850 hPa, 12Z

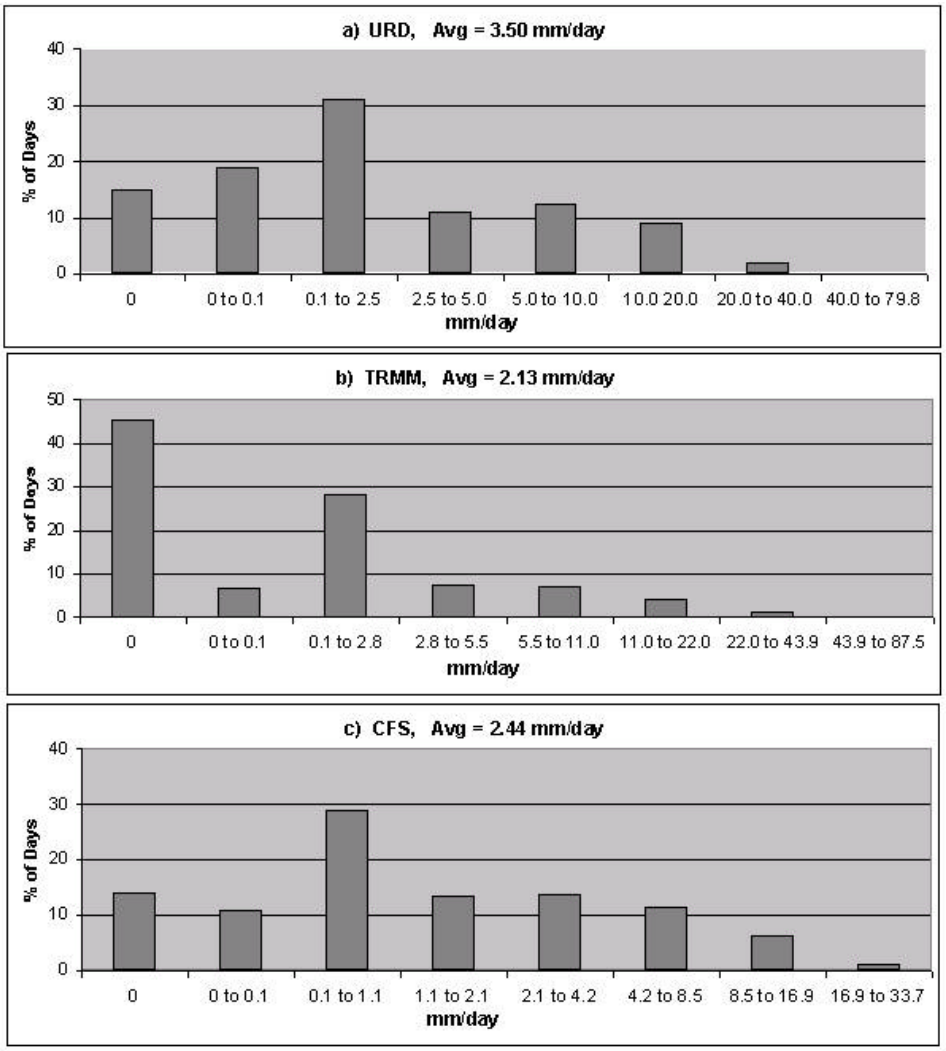

Figure 16. Frequency of daily rainfall rates in gridpoints within the CORE subregion, JJA 2004 [mm/d]. The y-axis shows the percentage of days for which daily rainfall at individual grid cells occurs within the range of values indicated underneath each bar. The first bar in each graph represents zero rainfall, and the second bar represents daily rainfall >0 mm but less than 0.1 mm. The next six bars represent ranges of daily rainfall scaled to the maximum daily value in the data, with the scaling the same for each graph.

a) URD observations
b) TRMM observations
c) CFS simulation